Beach placer, a proxy for the average Nd and Hf isotopic composition of a continental area

Marion Garçon, Catherine Chauvel, Sara Bureau

1

2

3

4

Beach placer, a proxy for the average Nd and Hf isotopic composition of a continental area

7

8

Marion Garçon[1], Catherine Chauvel[1], Sarah Bureau[1]

[1] ISTerre, CNRS, Université Joseph Fourier de Grenoble, BP 53, 38041 Grenoble Cedex 09, France

13

14

15

16

17

18

19

20

21

22

23

24

25   **Abstract**

26   Beach placer deposits concentrate detrital heavy minerals which are the erosion

27   products of large areas of continental crust. Here, we report the first analyses of Nd-Hf isotopic

28   ratios and trace element concentrations that we measured in a beach placer from Camargue,

29   France and in its pure mineral separates. Both the bulk composition of the placer and those of

30   its pure mineral separates were determined. We also report mineral proportions obtained using

31   observations under a binocular microscope and micro X-ray fluorescence mapping.

32   Our results indicate that monazite totally controls the placer's Nd isotopic composition

33   (ε_{Nd} = -9.3) while zircon dominates its Hf isotopes (ε_{Hf} = -13.0) even though both mineral phases

34   represent only a small proportion of the heavy mineral assemblage (3.5 and 10% respectively).

35   We demonstrate that the Camargue placer provides a good estimate of the average Nd and Hf

36   isotopic composition of the continental area drained by the Rhone River in western Europe (ε_{Nd}

37        $\approx$ -9 and $\varepsilon_{Hf} \approx$ -13). Using these values, we calculate two stage model ages and show that almost

38   all the placer minerals are derived from Proterozoic crustal protoliths. This provides valuable

39   information on the history of the continental crust drained by the Rhone River. In particular, it

40   suggests that little juvenile crust was created during the recent geological events that formed

41   the Alps and the Massif Central, the two main massifs from which the placer minerals originate.

42   More generally, we propose that similar measurements made on other worldwide beach

43   placer deposits could provide estimates of the present-day Nd and Hf isotopic composition of

44   large continental areas, values that are difficult to obtain due to the well-known heterogeneity

45   of continental material but are essential to model the growth of continental crust through Earth

46   history or to model the impact of crustal material when recycled into the mantle.

47

48   **Keywords:** Neodymium, hafnium, monazite, zircon, continental crust

49

1. Introduction

Modern beach placer deposits are surficial accumulations of clastic heavy minerals that mostly form in the foreshore of sandy beaches by gravity separation under the action of waves and currents. In some regions, beach placers contain valuable heavy minerals such as ilmenite, zircon or monazite and have been studied to identify economically viable deposits (e.g. Patyk-Kara, 2002; Levchenko, 2006; Patyk-Kara, 2008) or to better understand the mechanisms responsible for mineral sorting and depositional patterns (e.g. Komar and Wang, 1984; Frihy et al., 1995; Roy, 1999; Hughes et al., 2000; Hou et al., 2003; Paine et al., 2005). Apart from Götze and Lewis (1994) who studied a few trace elements in pure mineral fractions separated from mature quartz sands, no study has focused on the isotope and trace-element geochemistry of placers and their heavy minerals, even though this type of sediment obviously has the potential to provide valuable insights on broader issues such as fluvial transport processes, crust-mantle recycling or the composition of the upper continental crust.

Several previous studies (see for example, Goldstein and Jacobsen, 1988; Gaillardet et al., 1995; Allègre et al., 1996; Millot et al., 2004; Kamber et al., 2005) used river sediments as proxies to evaluate either the trace element content or the Nd and Pb isotopic compositions of the upper continental crust and its evolution through time. Other studies used Hf and Pb isotopes on individual zircon grains to constrain the timing of major crustal growth episodes as well as their mantle versus crustal sources (Gehrels et al., 1995; Amelin et al., 1999; Bodet and Schärer, 2000; Griffin et al., 2006; Hawkesworth and Kemp, 2006; Dhuime et al., 2011). However, no study ever considered taking advantage of the natural processes leading to the formation of zircon-rich placers to place constraints on both the composition and history of large-scale continental areas.

Here we present the first Nd and Hf isotopic analyses, as well as trace element concentrations, of several pure mineral separates that were isolated from a beach placer sampled

75   near the Rhone delta in Camargue, France. The proportion of each heavy mineral species was

76   estimated as precisely as possible using observations under a binocular microscope and micro

77   X-ray fluorescence mapping. Using all these data, we (a) quantify the influence of the individual

78   minerals on the trace element and isotopic composition of the entire placer, (b) we discuss and

79   interpret the chemical characteristics of beach placers and (c) we demonstrate that placers are

80   good proxies of the average Nd-Hf isotopic composition of large regions of the continental crust

81   exposed to weathering and erosion.

82

83   **2. Materials and Methods**

84   **2.1. Brief setting and placer sampling**

85   The studied placer was sampled in 2003 next to the Rhone River delta on the Espiguette

86   Beach in Camargue, France (see Figure 1) within the zone of wave swash where black-sand

87   deposits are regularly observed after storms. Several kilos of mature sand, rich in black heavy

88   minerals and mixed with very small proportions of light minerals, were collected using a spade

89   on the beach. Previous studies (BRGM, 2000) showed that the Espiguette black-sands usually

90   contain variable abundances of about twenty heavy minerals that are commonly found in beach

91   placer deposits. These include ilmenite, magnetite, rutile, garnet, zircon, monazite and epidote

92   (see Supplementary Table 1 for the complete list of minerals).

93   As shown in Figure 1, Espiguette beach is about 10 kilometres long and grows by

94   accumulation of sediments transported from east to west by longshore currents (Vella et al.,

95   2005; Sabatier et al., 2006). The accumulated sediments essentially originate from the

96   reworking of relict pro-deltaic lobes of the Rhone River and consist of materials directly eroded

97   from the massifs drained by the Rhone River and its tributaries. Several studies (BRGM, 2000;

98   Vassas et al., 2006) and more importantly the analyses of zircon typologies and apatite fission

99   track densities performed by Thomassin et al. (2007) demonstrated that the Alps and the Massif

4

100   Central are the two main sources for the heavy minerals that accumulate in the Camargue beach

101   placers.

102

103   **2.2. Separation of the mineral fractions**

104   Before analysis and mineral separation, the placer sand was washed, placed in an ultra-

105   sonic bath and oven-dried to remove organic material and seawater. Using heavy liquids

106   (bromoform and methylene iodide), the minerals were separated into three different fractions

107   according to their density. In the heaviest fraction (d > 3.3 g.cm^{-3}), the main minerals were

108   isolated according to their magnetic susceptibility using a hand magnet and a Frantz Isodynamic

109   Magnet Separator. Due to their similar magnetic properties, monazite, epidote and titanite were

110   relatively difficult to separate from one another. However, the epidote and titanite grains were

111   generally larger than the monazite grains and we separated them by collecting the fine and

112   coarse fractions after simple 80μm-sieving. The isolated fractions were then purified by

113   handpicking under a binocular microscope. We obtained six pure mineral separates consisting

114   of garnet, ilmenite, rutile, zircon, epidote and monazite. However, due to the optical similarities

115   of ilmenite and magnetite and because it is impossible to completely eliminate impurities with

116   a hand magnet, we suspect that the pure ilmenite separate likely refers to a fraction containing

117   a few magnetite grains.

118   **2.3. Heavy mineral abundances**

119   Mineral proportions were determined under a binocular microscope in a fraction

120   containing all the heavy minerals isolated from the Camargue placer (d > 2.9 g.cm^{-3}) using

121   standard optical characteristics such as grain colour or grain shape. In this heavy mineral

122   fraction, the mineral abundances were estimated as a percentage of the total counted grains.

123   As the identification of certain heavy minerals can be ambiguous in placers because of

124   altered or rounded grains, we also developed a method that uses micro X-ray fluorescence

125   mapping (μXRF EDAX Eagle III) to quantify the mineral abundances in the heavy fraction (d

126   > 2.9 g.cm³). Several hundred grains were analyzed by μXRF in order to identify their spectral

127   signature and their mineralogical characteristics (see Supplementary File B). Then, using this

128   information, we calculated the relative abundance of each mineral species as a percentage of

129   the total grains analysed by μXRF.

130   Combining the observations under the binocular microscope with the results obtained

131   by μ-XRF mapping, we estimated mineral abundances and converted them to mass percentage

132   using specific mineral densities and average grain sizes.

133

134   **2.4. Chemical analyses of the mineral fractions**

135   Trace element concentrations and Nd-Hf isotopic compositions were measured in bulk

136   fractions to evaluate the influence of each mineral on the geochemistry of the Camargue placer.

137   Measurements were performed on the six mineral separates (monazite, garnet, ilmenite, zircon,

138   epidote and rutile), the total placer and on two fractions, one containing all the light minerals

139   (d < 2.9 g.cm³) and the other containing all the heavy minerals (d > 2.9 g.cm³). To assess the

140   efficiency of the purification by handpicking under a binocular microscope, the impure

141   monazite, garnet, ilmenite and zircon fractions were also analysed.

142

143   *Sample dissolution*

144   The samples were first ground to fine powder by hand in an agate mortar to facilitate

145   dissolution. They were then dissolved by acid attack in steel PARR bombs for at least 2 weeks

146   at 135°C. Because of the well-known resistance of most placer minerals, we used sample-

147   specific dissolution procedures in which the sample quantity, the acid mixture and the

148   dissolution time in bombs were adapted to the mineral species (see Supplementary File C). In

149   addition, in order to improve the efficiency of the dissolution, acid-mixtures were regularly

150   removed from the bomb, stored in separated beakers and new acids were added every week.

151   After complete dissolution, two aliquots were taken from each dissolved sample, one to

152   measure trace element concentrations and the other for Nd-Hf isotopic compositions.

153

154   *Trace element concentrations*

155   Trace element concentrations were measured in mineral fractions using an Agilent

156   7500ce ICP-MS in Grenoble, France following a procedure similar to that published by Chauvel

157   et al. (2011). High precision measurements on ICP-MS were obtained by diluting samples in

158   2% HNO_3 with traces of HF at a specific dilution factor that depends on the sample and the

159   chemical element (see Supplementary File B). As described by Chauvel et al. (2011), ICP-MS

160   analytical drift was corrected by adding an internal standard (a multispike containing Be, Ge,

161   In, Tm, Bi) to all samples. After correction for drift and oxide interferences, trace element

162   concentrations were calculated using an external calibration based on the repeated

163   measurements of the BR rock standard diluted 5000 times. To ensure the validity and the

164   reproducibility of our measurements, rock standards AGV-1 and BR 24 were measured several

165   times as unknown samples and several duplicates were performed (see Supplementary Table 2

166   and 3).

167

168   *Nd and Hf isotopic compositions*

169   Following the method described by Chauvel et al. (2011), Hf and Nd were isolated from

170   the same aliquot using ion exchange resins. For the pure mineral separates, the Hf isolation

171   procedure was slightly modified since the standard method was not suitable for minerals that

172   are much more concentrated in trace elements than usual rocks or sediments (see

173   Supplementary File B). The total procedural blanks were always less than 20 pg for Nd and 120

174   pg for Hf and can thus be considered as negligible relative to the amount of Nd and Hf present

175 in the samples. Nd and Hf isotopic ratios were measured on a Nu Plasma MC-ICP-MS at the

176 ENS Lyon, France. The mass fractionation bias was corrected using the constant values of the

177 ratios $^{146}Nd/^{144}Nd=0.7219$ and $^{179}Hf/^{177}Hf=0.7325$. Analytical drift was monitored by measuring the

178 Ames-Rennes Nd and Ames-Grenoble Hf standards every two or three samples and was

179 corrected using the recommended values published by Chauvel and Blichert-toft (2001) and

180 Chauvel et al. (2011). These two standards yielded a mean $^{143}Nd/^{144}Nd$ value of 0.511962 ± 13

181 (2σ, n = 18) and $^{176}Hf/^{177}Hf$ value of 0.282160 ± 10 (2σ, n = 11).

182

183 **3. Results**

184 **3.1. Mineralogical composition of the heavy and light mineral fractions**

185 Using the weight of each separated fraction, we estimated that the light minerals (d <

186 2.9 g.cm^3) represent only 5% wt of the total placer whereas the heavy minerals (d > 2.9 g.cm^3)

187 constitute about 95% wt of the sample. Observation of the light mineral fraction under the

188 binocular microscope shows that it mainly contains calcite, feldspar and quartz, but also a few

189 residual heavy minerals (ilmenite, zircon, etc...) that were not properly separated from the light

190 minerals by the heavy liquid separation procedure. Figure 2 shows the mineral abundances in

191 the heavy mineral fraction determined under the binocular microscope and using the μXRF

192 mapping. The mineral proportions estimated by combining the results from the two methods

193 are given in the grey-coloured inset as a percentage of the total counted grains and as a mass

194 percentage. The uncertainties on the mineral proportions and the details about mass percentage

195 calculations are given in the Figure caption. As shown in Figure 2, the results obtained by μXRF

196 mapping are remarkably consistent with the observations done under the binocular microscope.

197 The heavy mineral fraction mainly contains ilmenite-magnetite (44%) and garnet (28%) but

198 also significant proportions of zircon (10%), rutile (7%), monazite (3.5%) and epidote (2%).

199   The μ-XRF determination provides precise abundances when the minerals are present

200   in significant proportions (> 5%) and has the advantage to be quick and inexpensive. However,

201   when the analysed grains have complex spectral signatures with too many peaks or variable

202   proportions of chemical elements, as is the case for garnet and epidote, the method cannot

203   accurately identify and quantify mineral abundances. In such a case, observation under the

204   binocular microscope provides better results. Unfortunately, for ilmenite and magnetite, both

205   methods remain inefficient because the two minerals are optically similar and their μ-XRF

206   spectral signatures are highly variable depending on the degree of alteration (Nair et al., 2009;

207   Suresh-Babu et al., 1994), hence indistinguishable with μ-XRF. The ilmenite percentage

208   calculated in the heavy mineral fraction is probably overestimated because it includes some

209   magnetite.

210

211   **3.2. Trace-element concentrations**

212   Trace-element concentrations measured in the placer, in the pure mineral separates and

213   in the light and heavy mineral fractions are given in Table 1 and concentrations in the impure

214   fractions of monazite, garnet, ilmenite and zircon are given in Supplementary Table 3. Except

215   for garnet, the composition of the impure fractions is similar to that of the pure mineral separate

216   but generally less concentrated in trace elements. To compare the composition of the entire

217   placer with that of the pure mineral separates and the light and heavy mineral fractions, the

218   concentrations of REE and other trace elements were normalized to the average chondrite

219   composition of Evensen et al. (1978) in Figure 3a and to the average upper continental crust

220   values of McLennan (2001) in Figure 3b. Compared to chondrites, the REE enrichment factors

221   span several orders of magnitude from 10 to almost 400 000 (Figure 3a). All samples are

222   characterised by a negative Eu anomaly. Compared to upper continental crust, enrichment

223   factors range from about 0.01 to 4000 (Figure 3b) and almost all samples display significant

224 depletions in Cs, Rb, Ba, Sr and Li elements that are all known to be highly mobile during

225 alteration.

226   As can be seen in Figure 3b, trace-element concentrations measured in the total placer

227 are about 100 times those of upper continental crust and are quasi-similar to those of the heavy

228 mineral fraction. In contrast, the light mineral fraction has much lower trace element

229 concentrations, quite similar to upper continental crust values. These three fractions display the

230 same small negative anomalies in Nb, Ta and positive anomalies in Hf and Zr (Figure 3b).

231   Except for garnet, trace-element concentrations measured in the pure mineral separates

232 strongly resemble those published in the literature when available and/or are consistent with

233 partition coefficients determined in many studies.

234 •   Monazite is extremely rich in Th-U and all REE but particularly the light REE (LREE)

235   (e.g. Kamineni et al., 1991; Ayres and Harris, 1997; Zhu and O'Nions, 1999; Nagy et

236   al., 2002; Thöni et al., 2008; Radulescu et al., 2009).

237 •   Ilmenite is characterized by positive anomalies in Nb-Ta that are consistent with the

238   partition coefficients determined by Klemme et al. (2006) and Melluso et al. (2008) for

239   these two elements.

240 •   Rutile and epidote display quite similar trace-element concentrations except for their

241   anomalies in Nb-Ta and in Zr-Hf which are positive for rutile and negative for epidote.

242   These features are in agreement with the partition coefficients determined by Foley et

243   al. (2000) and Klemme et al. (2005) for these four elements.

244 •   Zircon differs from other minerals because of its strong depletion in LREE and its

245   significant enrichment in Hf and Zr (Figure 3; see Hoskin and Schaltegger, 2003 for a

246   review).

247 •   Garnet is more enriched in HREE than in LREE (Figure 3a), displays unusual positive

248   Zr and Hf anomalies (Figure 3b) and its LREE concentrations are not as low as usually

249	measured in typical metamorphic or magmatic garnets (Jung and Hellebrand, 2006). In
250	the pure garnet separate, the higher LREE concentrations associated with the Hf and Zr
251	anomalies might be due to the presence of zircon inclusions and/or to an incomplete
252	sorting of the fraction.
253	
254	**3.3. Nd and Hf isotopic compositions**
255	Nd and Hf isotopic ratios measured in the placer, the pure mineral separates and the
256	heavy and light mineral fractions are given in Table 2 and are plotted in a ε_{Hf} vs. ε_{Nd} diagram in
257	Figure 4. The isotopic compositions of the impure fractions of monazite, garnet, ilmenite and
258	zircon are given in Supplementary Table 3. Except for garnet, the compositions of the impure
259	separates resemble those of their respective pure mineral separates. Nd and Hf isotopic
260	compositions measured in the placer, the pure mineral separates and the heavy and light mineral
261	fractions span a large range of values from 0.512150 (ε_{Nd} = -9.4) to 0.512594 (ε_{Nd} = -0.7) for Nd
262	and from 0.282358 (ε_{Hf} = -15.1) to 0.282942 (ε_{Hf} = +5.6) for Hf. The pure zircon separate has
263	the highest Nd isotopic ratio and one of the lowest Hf isotopic ratios whereas the pure monazite
264	separate has the highest Hf isotopic ratio and one of the lowest Nd isotopic ratios. Considering
265	the analytical uncertainties on the measurements, the total placer, the rutile and the light and
266	heavy mineral fractions have similar Nd and Hf isotopic compositions which all lie on the
267	mantle array in the ε_{Hf} vs. ε_{Nd} diagram (Figure 4). Ilmenite and garnet have more radiogenic Nd
268	and Hf isotopic ratios that also fall on the mantle array in Figure 4. In contrast, epidote lies well
269	above the mantle array due to the radiogenic decay associated to its high Lu/Hf ratio.
270	
271	**4. Discussion**
272	**4.1. Geochemical characteristics of the Camargue placer**

273   As heavy minerals are important carriers of trace elements (e.g. Götze and Lewis, 1994;

274   Preston et al., 2002; Totten and Hanan, 2007), we first decipher the contribution of each mineral

275   species to the overall chemistry of the Camargue placer in order to further investigate the Sm-

276   Nd and Lu-Hf systematics of beach placers.

277

278   *4.1.1. The heavy minerals control the trace element budget of the placer*

279   In Figure 5, we normalised the trace element concentrations of the heavy (high density,

280     $d > 2.9$ g.cm^{-3}) and light (low density, $d < 2.9$ g.cm^{-3}) mineral fractions to the bulk composition

281   of the Camargue placer to assess their respective contributions to the chemical budget of the

282   placer. The enrichment factors calculated for the heavy mineral fraction are very close to 1

283   whereas they are quite low for the light mineral fraction - usually < 0.1. This clearly shows that

284   heavy minerals almost totally control the bulk geochemistry of the placer by hosting most trace

285   elements. Except for some mobile elements such as Cs, Rb, Ba, Sr and Li, the light minerals do

286   not sequester large amounts of trace elements. The very low concentrations measured in this

287   fraction indicate that it contributes to very little of the overall chemical budget of the placer but

288   it still has the potential to significantly dilute overall concentrations (Götze and Lewis, 1994;

289   Vervoort et al., 1999). We also see that the spectrum for the light mineral fraction in Figure 3b

290   is not really consistent with those usually found in the literature for quartz, feldspar or calcite,

291   the main mineral species present in this fraction (see Götze and Lewis, 1994; Govindaraju,

292   1994; Korotev, 1996; Monecke et al., 2000; Strnad et al., 2009). The light mineral fraction

293   displays unusual HFSE contents that strongly resemble those found in the heavy mineral

294   fraction (negative anomaly in Nb and Ta and positive anomaly in Zr and Hf, see Figure 3). This

295   feature is best explained by the presence of few heavy minerals in the light mineral fraction, a

296   feature not surprising since, unlike the pure mineral separates analysed in this study, the light

297   mineral fraction was not carefully purified by hand-picking under a binocular microscope.

298

4.1.2. Trace elements hosted by pure mineral separates

299

In Figure 5, the placer-normalised patterns reflect the contribution of each heavy mineral

300

to the bulk trace-element budget of the placer. With its very high concentrations, monazite

301

obviously is the major carrier of Th, U and REE. Zircon mainly controls Zr, Hf and to a lesser

302

extent U and HREE while rutile and ilmenite host most Nb and Ta in the placer. The other trace

303

elements such as Cs, Rb, Ba, Sr, Pb or Li are carried in variable proportions by several mineral

304

species and their concentrations in the total placer are not controlled by one or two specific

305

mineral species (Figure 5).

306

To ensure that we isolated and analysed all the heavy mineral species that significantly

307

contribute to the trace-element budget of the placer, we use the concentrations measured in the

308

pure mineral separates and the mineral proportions estimated as mass percentages in Figure 2

309

to calculate a theoretical trace element pattern for the heavy mineral fraction. In Figure 6, we

310

compare it to the measured values. We also take into account the uncertainties estimated on the

311

mineral proportions (see footnote of Figure 6 for more detail) and we model a field of variability

312

for the calculated heavy mineral fraction concentrations (blue field in Figure 6). With the

313

exception of the HREE and some mobile elements, our results show that the measured trace-

314

element pattern of the heavy mineral fraction is extremely well reproduced using the combined

315

proportions of pure monazite, zircon, ilmenite, garnet, rutile and epidote. This confirms that,

316

except for the HREE, the pure mineral separates account for the trace element budget of the

317

heavy mineral fraction. For Nd and Hf, our calculation shows that their concentrations in the

318

heavy mineral fraction are completely reproduced using only the mass proportions and contents

319

measured in the pure monazite and zircon separates. Other minerals play close to no role in the

320

overall abundance of Nd and Hf in the heavy mineral fraction. Monazite contains such high

321

amounts of LREE and zircon such high amounts of Zr and Hf that even though they constitute

322

323   only small percentages of the mineral assemblage, they are the controlling carriers of Nd and

324   Hf in the beach placer. Finally, we interpret the misfit between calculated and measured

325   concentrations for Cs, Rb, Ba and heavy REE (Figure 6) as being due to impurities in the garnet

326   separate and/or to the presence of a mineral such as titanite, which we did not separate and

327   analyse.

328

329   *4.1.3. What controls the Nd and Hf isotopic systematic of beach placer?*

330   Given that monazite and zircon are the carriers of Nd and Hf in the placer, they should

331   control the isotopic compositions. To confirm this hypothesis, we calculated a mixing curve

332   between these two minerals using the equation established by Faure (1977). This mixing curve

333   and the mass proportion of monazite in the binary mixture are shown in Figure 4. Because

334   monazite controls the Nd content and zircon the Hf content, the mixing hyperbola has such a

335   strong curvature that it resembles two perpendicular straight lines in the ε_{Hf} vs. ε_{Nd} diagram. The

336   first important observation is that, within uncertainties, the bulk composition of the placer, as

337   well as those of the light and heavy mineral fractions plot at the point of maximum curvature

338   on the mixing curve. A simple binary mixture of monazite and zircon without all the other

339   mineral species thus properly reproduces their Nd and Hf isotopic compositions. This confirms

340   that monazite totally controls the Nd isotopic composition in the placer as well as that of the

341   heavy and the light mineral fractions while zircon totally dominates the Hf isotopic

342   composition.

343   As a consequence of the concentration contrast between monazite and zircon for Nd and

344   Hf, the proportion of monazite in the monazite-zircon mixture varies widely near the point of

345   maximum curvature on the hyperbola (see the inset of Figure 4). Considering an uncertainty of

346   0.7 ε units on the isotopic compositions, mixing calculations demonstrate that as long as there

347   is 5 to 90% of monazite in the monazite-zircon mixture, the ε_{Nd} of the mixture remains similar

14

348   to that of the monazite and the ε_{Hf} to that of the zircon. A very wide range of monazite-zircon

349   ratio will thus produce Nd and Hf isotopic compositions that lie at the point of maximum

350   curvature on the mixing hyperbola. This, together with the fact that heavy mineral proportions

351   determined in the studied Camargue placer are comparable to those usually found in mature

352   beach placer deposits, make us very confident in the reproducibility of our results. Hence, we

353   are convinced that similar isotopic compositions would characterize placer samples taken from

354   various locations on the same beach even if heavy mineral proportions vary locally.

355   This latter observation potentially has major implications for beach-placer deposits in

356   other parts of the world. Indeed, monazite and zircon are very common minerals in most

357   coastal-marine placers (Patyk-Kara and Shevelev, 2000; Patyk-Kara, 2002) where they

358   represent 1-5 wt% and 5-20 wt% of the heavy mineral assemblage, respectively (e.g. Carpenter

359   and Carpenter, 1991; Force, 1991; Rao, 1994; Roy, 1999; Paine et al., 2005; Levchenko, 2006),

360   proportions that are comparable to those estimated in the Camargue placer. Given that zircon

361   is unequivocally the major carrier of Hf among common heavy minerals, we suggest that, as

362   for the Camargue placer, the Hf elemental and isotopic budget of worldwide beach placers is

363   likely entirely controlled by zircon. For Nd content and isotopic composition, the situation is

364   more ambiguous because the percentage of monazite in the heavy mineral assemblages can

365   sometimes be low and other minerals will influence the placer Nd isotopic composition if they

366   are present in sufficiently large proportions. Apatite probably constitutes the most serious

367   competitor to monazite in the REE budget of placers because it contains significant amounts of

368   REE and is sometimes present at the percent level in some beach placers. However, the normal

369   Nd content of monazite is at least 100 times that of typical apatite (see Ayres and Harris, 1997

370   and Belousova et al., 2002 for Nd concentrations in apatites) and 1000 times that of other

371   common placer minerals (cf Figure 3a; Götze and Lewis, 1994). A simple calculation shows

372   that even if a placer contains only 0.5% monazite, 5% apatite and 94.5% other minerals, 80%

373   of the overall Nd budget is still control by monazite. We therefore suggest that the Nd and Hf

374   isotopic compositions of worldwide beach placers should be controlled by monazite and zircon

375   even though their abundances in the heavy mineral assemblage are often low.

376

377   **4.2. Present-day Nd and Hf isotopic compositions of continental areas**

378   *4.2.1. The continental area drained by the Rhone River*

379   Previous studies showed clearly that the present-day Hf-Nd isotopic compositions of

380   crustal rocks plot on the extension of the mantle array in a Hf-Nd isotopic space and thus on

381   the same trend as rocks coming from the mantle (Vervoort and Patchett, 1996; Vervoort et al.,

382   1999; Vervoort et al., 2000) (Figure 4). In Figure 4, data for the Camargue placer lie on the

383   mantle array and also fall in the field of crustal rocks, suggesting that its present-day ε_{Nd} at -9

384   and its ε_{Hf} at -13 are quite comparable to that of continental crust materials. Our ε_{Hf} value is the

385   first published estimate for the Hf isotopic composition of crustal rocks from Western Europe

386   since no Hf data are available for the source rocks in the region drained by the Rhone River.

387   This is not the case for ε_{Nd}, however. Figure 7 shows that our ε_{Nd} value is identical to the average

388   value calculated from a compilation of ε_{Nd} reported in the literature for continental crust rocks –

389   granitoids and orthogneiss essentially – from the Massif Central and the Western and Central

390   Alps. It also corresponds to the average Nd isotopic composition of metamorphic rocks,

391   sediments and granitoids of the Hercynian fold belt of Central Europe (Liew and Hofmann,

392   1988). We conclude that the placer's Nd and Hf isotopic compositions represent those of the

393   average source region of the sediment, allowing us to provide the following estimate for the

394   Western European crust: $\varepsilon_{Hf} \approx -13$ and $\varepsilon_{Nd} \approx -9$.

395

396   *4.2.2. Can beach placers be used as proxies for other continental areas?*

397   While we believe that the Camargue placer might be a good proxy for the average Nd

398   and Hf isotopic composition of the continental area drained by the Rhone river, this might not

399   be the case for other beach placers. For an estimate based on placer data to be robust requires a

400   number of conditions that we will now examine. We demonstrated above that the Nd and Hf

401   isotopic compositions of the Camargue placer are controlled by monazite and zircon, ubiquitous

402   minerals that host most of the LREE and Hf in crustal rocks. However, it is also known that

403   parent/daughter ratios such as Sm/Nd and Lu/Hf change when minerals crystallize from a

404   magma (Faure, 1977) and that sedimentary rocks do not necessarily have the same ratios as

405   their sources (Patchett et al., 1984). As time passes after formation of the minerals, the isotopic

406   compositions of minerals evolve following their parent/daughter ratios, which might be

407   significantly different from those of the whole rock. The impact of the difference in

408   parent/daughter ratio needs therefore to be quantitatively evaluated before we can conclude that

409   placers represent proxies for the average Nd and Hf isotopic composition of their crustal

410   precursors.

411   In continental crust granitoids, Nd resides not only in monazite but also in other minerals

412   such as apatite, allanite or feldspar (Taylor and McLennan, 1995; Bea, 1996) that are not

413   systematically concentrated in beach placers when continental crust is eroded. Nevertheless, as

414   for most common granite-forming minerals (e.g. Taylor and McLennan, 1995; Bayon et al.,

415   2006), monazite has the same $^{147}Sm/^{144}Nd$ ratio as continental crust (see McLennan, 2001 and

416   Rudnick and Gao, 2003 for continental crust ratios and Ayres and Harris, 1997; Thöni et al.,

417   2008 and our own measurement for monazite ratios). Consequently, the monazite Nd isotopic

418   composition never significantly differs from that of crustal rocks and can be considered as a

419   good estimate of the average crustal value even if monazite does not dominate the Nd content

420   of crustal rocks. In contrast, most of the Hf in continental crust granitoids is hosted in resistant

421   zircons (Patchett et al., 1984; Candela, 2003), which have low $^{176}Lu/^{177}Hf$ ratios compared to that

422   of continental crust (0.002 versus 0.013) (see McLennan, 2001 and Rudnick and Gao, 2003 for

423   continental crust ratios and Kinny and Maas, 2003 for zircon ratios). As a consequence,

424   significant isotopic differences develop between mineral and crustal precursor if the zircon

425   crystallization age is old. In practice, using a $^{176}Lu/^{177}Hf$ ratio of 0.002 for the zircon and 0.013

426   for the continental crust, our calculations show that if the zircon crystallization age is younger

427   than 500 Ma, its isotopic composition differs from that of its crustal precursor by less than two

428   ε_{Hf}. This is simply because time is not sufficient for the difference in Lu/Hf to produce a Hf

429   isotopic composition in the zircon very different from that of the crust. As a result, the Hf

430   isotopic composition of a young zircon population, such as that in the Camargue placer, can be

431   considered as a valuable proxy for the average crustal value of the drained area. In the case of

432   an older zircon population, a correction could be applied provided that the average age of the

433   population is known.

434   In summary, we believe that placers have the potential to provide naturally averaged

435   information about the isotopic composition of large portions of the crust exposed to weathering

436   and erosion, information that is not always available as revealed by the numerous papers that

437   aim to estimate the composition of the continental crust (e.g. Taylor and McLennan, 1995;

438   McLennan, 2001; Rudnick and Gao, 2003). Although we recognize that analytical procedure,

439   particularly for sample dissolution, is sometimes difficult, we suggest that analyses of

440   worldwide beach placer deposits may constitute a fairly simple way to constrain the Nd-Hf

441   systematics of large continental areas. We recognize that this estimate does not take into

442   account mafic and ultramafic materials that could exist in the drainage area because monazite

443   and zircon, the two minerals controlling the Nd and Hf isotopic compositions of beach placers,

444   are not ubiquitous in mafic and ultramafic rocks. Beach placer deposits approximate therefore

445   the average isotopic composition of materials of continental affinity. Interesting sampling sites

446   could be the deltas of large rivers where vast amounts of terrigenous material are deposited and

447   where sea currents facilitate the formation of heavy mineral concentrates (Komar, 2007).

448

449   **4.3. Nd and Hf model ages of the drained continental area**

450   *4.3.1. Two stage model age calculations*

451   Since minerals do not necessarily have Sm/Nd and Lu/Hf ratios similar to those of their

452   whole rocks, Nd and Hf model ages of their crustal protolith must be calculated using a two

453   stage-model, a first stage for the time spent in the crust and a second for the evolution of the

454   mineral itself since crystallisation. For this calculation, we assume that the Sm-Nd and Lu-Hf

455   isotopic systems evolved first in a continental crust-type reservoir extracted from the depleted

456   mantle and then, after crystallisation, in the minerals themselves. An example of the calculation

457   for the Lu-Hf isotopic system is shown in Figure 8 and the calculated Hf model ages are shown

458   as a function of the Nd model ages in Figure 9. For the placer and for each mineral fraction,

459   model ages were estimated using a Monte-Carlo procedure to propagate uncertainties related to

460   (1) the isotopic composition of the depleted mantle (mean MORB-pole from the compilation

461   made by Chauvel et al., 2008), (2) the $^{147}Sm/^{144}Nd$ and $^{176}Lu/^{177}Hf$ ratios of average continental crust

462   and (3) the crystallisation ages of the placer minerals (see caption of Figure 9 for more details).

463   As a primary hypothesis, we considered that the crystallisation age of all minerals were, on

464   average, Hercynian (300 ± 50 (2σ) Ma) given that (1) this period corresponds to the last major

465   magmatic event forming widespread plutonic bodies and occurring both in the Eastern Massif

466   Central and in the Western Alps (Pin and Duthou, 1990; Debon and Lemmet, 1999), the two

467   main sources of the placer minerals and (2) numerous studies have reported crystallisation ages

468   between 290 Ma and 340 Ma for monazite and zircon populations from the Massif Central and

469   the Western-Central Alps (e.g. Bossart et al., 1986; Sergeev et al., 1995; Bruguier et al., 2003;

470   Mezeme et al., 2006; Rossi et al., 2006; Gébelin et al., 2009). Using this assumption, similar

471   model ages are calculated for the two isotopic systems for the placer, the light and heavy

472   mineral fractions and for each pure mineral separate, as shown by the distribution in Figure 9.

473   In contrast, if we assume an average Alpine crystallisation age of about 30-50 Ma or any age

474   younger than 250 Ma or older than 350 Ma, large discrepancies occur between the Nd and Hf

475   model ages. This would imply a systematic decoupling of the Sm-Nd and Lu-Hf isotopic

476   systems in every mineral species, a situation that is obviously unrealistic. As an example for

477   the pure zircon separate, taking a crystallisation age of 50 Ma leads to Nd model ages (0.7 to 1

478   Ga) much younger than the Hf model ages (1.3 to 1.7 Ga) while taking a crystallisation age of

479   500 Ma provides Nd model ages (1.7 to 2.0 Ga) that are far older than the Hf model ages (1.2

480   to 1.5 Ga). We are therefore confident that calculating model ages using a mean crystallisation

481   age of 300 ± 50 (2σ) Ma for all the placer minerals provides robust information about the Nd

482   and Hf isotopic systematics of the source region. Note that the bulk placer and some of the

483   mineral fractions, such as the light and heavy mineral fractions, the pure ilmenite for Hf and

484   the pure rutile for Nd, have parent/daughter ratios that resemble those of the continental crust,

485   hence they have robust model ages that do not depend on the age of crystallisation we chose to

486   calculate them.

487

488   *4.3.2. Implications for the history of the drained continental area*

489   Almost all mineral fractions, and the placer itself, display consistent Nd and Hf model

490   ages (Figure 9) grouped around 1.4 - 1.5 Ga, suggesting that they derive from similar crustal

491   protoliths. The only exceptions are epidote and ilmenite both of which are characterised by

492   slightly younger ages around 1.1 to 1.3 Ga. Assuming a younger crystallisation age for these

493   two minerals does not significantly raise the Hf and Nd model ages. As a consequence, epidote

494   and ilmenite may record more recent geological events or their parent/daughter ratios may have

495   been disturbed by secondary processes.

20

496   Our calculated Nd and Hf model ages are fully consistent with the Proterozoic Nd model

497   ages reported for granitoids from the Massif Central and the Alps (e.g. Bossart et al., 1986;

498   Paquette et al., 1989; Downes et al., 1990) and strongly resemble those of metamorphic rocks,

499   sediments and granitoids from the European Hercynian fold belt whose model ages vary mainly

500   between 1.4 and 1.7 Ga (Liew and Hofmann, 1988). This suggests that the bulk composition of

501   the Camargue placer provides a true estimate of both the Nd and Hf model ages of the large

502   continental area drained by the Rhone River. More generally, Nd and Hf model ages obtained

503   on placer sands from continents could provide similar information for the crustal evolution of

504   large continental areas.

505   According to our measurements and calculations, the mean crustal residence age of the

506   Nd and Hf now residing in the Camargue placer minerals is Proterozoic, hence far older than

507   the age of the main orogenies that produced the Hercynian and Alpine terranes. As discussed

508   by many authors studying the Hercynian magmatism in the Massif Central and the Alps (e.g.

509   Bossart et al., 1986; Paquette et al., 1989; Pin and Duthou, 1990; Sergeev et al., 1995; Downes

510   et al., 1997), such model ages are best explained in terms of a two-component mixing between

511   new crust and an older component at least Early Proterozoic in age. This suggests strongly that

512   the main process occurring during the Hercynian and Alpine orogenies was reworking of old

513   continental crust with little addition of new material. Considering that the mean age of the old

514   crustal component is 1.8 - 2.0 Ga (Peucat et al., 1988) and that of the placer minerals is about

515   1.5 Ga, a simple calculation shows that a maximum of 20 - 30% juvenile crust could have been

516   added over the last 400 Ma i.e. during the recent Hercynian and Alpine events. Both Sm-Nd

517   and Lu-Hf isotopic systems thus record clear evidence that the continental area drained by the

518   Rhone River had a long history prior to the known Hercynian and Alpine events and that large

519   amounts of old crustal material with a mean Proterozoic age were reworked during the genesis

520   of rocks currently forming the Massif Central and the Alps.

521

5. Conclusions

522

523   This study provides the first analyses of Nd and Hf isotopes and associated trace element

524   concentrations for a placer and the main mineral species it contains. Our results show that heavy

525   minerals host most trace elements while light minerals only dilute concentrations. More

526   specifically, we show that monazite and zircon control the Nd and Hf isotopic compositions,

527   respectively, of the Camargue placer. A simple mixture of only these two minerals reproduces

528   not only the isotopic compositions but also the Nd and Hf concentrations of the bulk placer. As

529   the mass percentages of heavy minerals in the studied placer are typical of those commonly

530   found in worldwide beach placer deposits, we suggest that monazite and zircon always

531   dominate the Nd and Hf isotopic compositions of beach placer even though they are usually

532   present in low proportions in the mineral assemblage.

533   Our data indicate that present-day Nd-Hf isotopic compositions of the Camargue placer

534   are representative of the crustal rocks found in the Massif Central and the Alps and provide

535   therefore a reliable estimate of the average isotopic composition of the continental area drained

536   by the Rhone River ($\varepsilon_{Nd} \approx$ -9, $\varepsilon_{Hf} \approx$ -13). The calculated Nd and Hf model ages for all placer

537   minerals are consistent and provide an average Proterozoic age for the history of this part of the

538   continental crust. We finally suggest that other beach placers formed at the mouths of large

539   rivers in other parts of the world could provide reliable estimates of the average Nd-Hf

540   compositions of other large continental areas, values that are usually not easy to obtain.

541

22

551

References

553 Allègre C J, Dupré B, Négrel P and Gaillardet J. 1996. Sr-Nd-Pb isotope systematics in Amazon

554   and Congo River systems: constraints about erosion processes. *Chemical Geology*

555   **131**(1-4): 93-112.

556 Amelin Y, Lee D C, Halliday A N and Pidgeon R T. 1999. Nature of the Earth's earliest crust

557   from hafnium isotopes in single detrital zircons. *Nature* **399**(6733): 252-255.

558 Ayres M and Harris N. 1997. REE fractionation and Nd-isotope disequilibrium during crustal

559   anatexis: constraints from Himalayan leucogranites. *Chemical Geology* **139**: 249-269.

560 Bayon G, Vigier N, Burton K W, Brenot A, Carignan J, Etoubleau J and Chu N-C. 2006. The

561   control of weathering processes on riverine and seawater hafnium isotope ratios.

562   *Geology* **34**(6): 433-436.

563 Bea F. 1996. Residence of REE, Y, Th and U in Granites and Crustal Protoliths; Implications

564   for the Chemistry of Crustal Melts. *Journal of Petrology* **37**(5): 521-552.

565 Belousova E A, Griffin W L, O'Reilly S Y and Fisher N I. 2002. Apatite as an indicator mineral

566   for mineral exploration: trace-element compositions and their relationship to host rock

567   type. *Journal of Geochemical Exploration* **76**: 45-69.

568 Bennett V C, Nutman A P and McCulloch M T. 1993. Nd isotopic evidence for transient, highly

569   depleted mantle reservoirs in the early history of the Earth *Earth and Planetary Science*

570   *Letters* **119**: 299-317.

571 Blichert-Toft J, Chauvel C and Albarède F. 1997. Separation of Hf and Lu for high-precision

572   isotope analysis of rock samples by magnetic sector-multiple collector ICP-MS.

573   *Contributions to Mineralogy and Petrology* **127**: 248-260.

574 Bodet F and Schärer U. 2000. Evolution of the SE-Asian continent from U-Pb and Hf isotopes

575   in single grains of zircon and baddeleyite from large rivers. *Geochimica et*

576   *Cosmochimica Acta* **64**(12): 2067-2091.

577 Bossart P J, Meier M, Oberli F and Steiger R H. 1986. Morphology versus U-Pb systematics in

578   zircon: a high-resolution isotopic study of a zircon population from a Variscan dike in

579   the Central Alps. *Earth and Planetary Science Letters* **78**: 339-354.

580 Bouvier A, Vervoort J D and Patchett J. 2008. The Lu–Hf and Sm–Nd isotopic composition of

581   CHUR: Constraints from unequilibrated chondrites and implications for the bulk

582   composition of terrestrial planets. *Earth and Planetary Science Letters* **273**: 48-57.

583 BRGM (2000). Expertise géologique des anomalies radioactives des plages de Camargue**:** 21

584   p.

585 Bruguier O, Becq-Giraudonb J F, Champenoisc M, Deloulec E, Luddenc J and Manginc D.

586   2003. Application of in situ zircon geochronology and accessory phase chemistry to

587   constraining basin development during post-collisional extension: a case study from the

588   French Massif Central. *Chemical Geology* **201**: 319-336.

589 Candela, P.A. 2003. Ore in the Earth's Crust. pp 411-431. In *The Crust* (ed. R.L. Rudnick)

590   *Vol. 3, Treatise on Geochemistry* (eds. H.D. Holland and K.K. Turekian), Elsevier-

591   Pergamon, Oxford.

592 Carpenter R H and Carpenter S F. 1991. Heavy Mineral Deposits in the Upper Coastal Plain of

593   North Carolina and Virginia. *Economic Geology* **86**: 1657-1671.

594 Chauvel C and Blichert-Toft J. 2001. A hafnium isotope and trace element perspective on

595   melting of the depleted mantle. *Earth and Planetary Science Letters* **190**: 137-151.

596   Chauvel C, Bureau S and Poggi C. 2011. Comprehensive chemical and isotopic analyses of

597   basalt and sediment reference materials. *Geostandards and Geoanalytical Research* **35:**

598   125-143.

599   Chauvel C, Lewin E, Carpentier M and Arndt N T. 2008. Role of recycled oceanic basalt and

600   sediment in generating the Hf-Nd mantle array. *Nature Geoscience* **1**: 64-67.

601   Debon F and Lemmet M. 1999. Evolution of the Mg/Fe Ratios in Late Variscan Plutonic Rocks

602   from the External Crystalline Massifs of the Alps (France, Italy, Switzerland). *Journal*

603   *of Petrology* **40**(7): 1151-1185.

604   Deer W A, Howie R A and Zussman J. 1992. *An Introduction to the Rock-Forming Minerals*.

605   Dhuime B, Hawkesworth C J, Storey C D and Cawood P A. 2011. From sediments to their

606   source rocks: Hf and Nd isotopes in recent river sediments. *Geology* **39**(4): 407-410.

607   Downes H. 1984. Sr and Nd isotope geochemistry of coexisting alkaline magma series, Cantal,

608   Massif Central, France. *Earth and Planetary Science Letters* **69**: 321-334.

609   Downes H, Dupuy C and Leyreloup A F. 1990. Crustal evolution of the Hercynian belt of

610   Western Europe: evidence for lowercrustal granulitic xenoliths (French Massif Central).

611   *Chemical Geology* **83**: 209-231.

612   Downes H and Duthou J L. 1988. Isotopic and trace element arguments for the lower crustal

613   origin of Hercynian granitoids and pre-Hercynian orthogneisses, Massif Central

614   (France). *Chemical Geology* **68**: 291-308.

615   Downes H, Shaw A, Williamson B J and Thirlwall M F. 1997. Sr, Nd and Pb isotopic evidence

616   for the lower crustal origin of Hercynian granodiorites and monzogranites, Massif

617   Central, France. *Chemical Geology* **136**: 99-122.

618   Duchene S, Blichert-Toft J, Luais B, Telouk P, Lardeaux J M and Albarede F. 1997. The Lu-

619   Hf dating of garnets and the ages of the Alpine high-pressure metamorphism. *Nature*

620   **387**(6633): 586-589.

621   Eggins S M, Woodhead J D, Kinsley L P J, Mortimer G E, Sylvester P, McCulloch M T, Hergt

622   J M and Handler M R. 1997. A simple method for the precise determination of > 40

623   trace elements in geological samples by ICPMS using enriched isotope internal

624   standardisation. *Chemical Geology* **134**: 311-326.

625   Evensen N M, Hamilton P J and O'Nions R K. 1978. Rare earth abundances in chondritic

626   meteorites. *Geochimica Cosmochimica Acta* **42**: 1199-1212.

627   Faure G. 1977. *Principles of isotope Geology* Wiley: New York.

628   Foley S F, Barth M G and Jenner G A. 2000. Rutile/melt partition coefficients for trace elements

629   and an assessment of the influence of rutile on the trace element characteristics of

630   subduction zone magmas. *Geochimica et Cosmochimica Acta* **64**(5): 933-938.

631   Force E R. 1991. *Geology of titanium-mineral deposits* Boulder, Colo. : Geological Society of

632   America.

633   Frihy O E, Lotfy M F and Komar P D. 1995. Spatial variations in heavy minerals and patterns

634   of sediment sorting along the Nile Delta, Egypt. *Sedimentary Geology* **97**(1-2): 33-41.

635   Gaillardet J, Dupré B and Allègre C J. 1995. A global geochemical mass budget applied to the

636   Congo basin rivers: Erosion rates and continental crust composition. *Geochimica et*

637   *Cosmochimica Acta* **59**(17): 3469-3485.

638   Gébelin A, Roger F and Brunel M. 2009. Syntectonic crustal melting and high-grade

639   metamorphism in a transpressional regime, Variscan Massif Central, France.

640   *Tectonophysics* **in press**.

641   Gehrels G E, Dickinson W R, Ross G M, Stewart J H and Howell D G. 1995. Detrital zircon

642   reference for Cambrian to Triassic miogeoclinal strata of western North America.

643   *Geology* **23**(9): 831-834.

644   Goldstein S J and Jacobsen S B. 1988. Nd and Sr isotopic systematics of river water suspended

645   material: implications for crustal evolution. *Earth and Planetary Science Letters* **87**(3):

646   249-265.

647   Götze J and Lewis R. 1994. Distribution of REE and trace elements in size and mineral fractions

648   of high-purity quartz sands. *Chemical Geology* **114**: 43-57.

649   Govindaraju K. 1994. 1994 Compilation of working values and sample description for 383

650   geostandards *Geostandards Newsletter* **18**: 1-158.

651   Griffin W L, Belousova E A, Walters S G and O'Reilly S Y. 2006. Archaean and Proterozoic

652   crustal evolution in the Eastern Succession of the Mt Isa district, Australia: U-Pb and

653   Hf-isotope studies of detrital zircons. *Australian Journal of Earth Sciences* **53**: 125-149.

654   Hawkesworth C J and Kemp A I S. 2006. Using hafnium and oxygen isotopes in zircons to

655   unravel the record of crustal evolution. *Chemical Geology* **226**(3-4): 144-162.

656   Henry P, Deloule E and Michard A. 1997. The erosion of the Alps: Nd isotopic and geochemical

657   constraints on the sources of the peri-Alpine molasse sediments. *Earth and Planetary*

658   *Science Letters* **146**: 627-644.

659   Hoskin P W O and Schaltegger U. 2003. The Composition of Zircon and Igneous and

660   Metamorphic Petrogenesis. *Reviews in mineralogy and geochemistry* **53**: 27 -62

661   Hou B, Frakes L A, Alley N F and Heithersay P. 2003. Evolution of beach placer shorelines

662   and heavy-mineral deposition in the eastern Eucla Basin, South Australia. *Australian*

663   *Journal of Earth Sciences* **50**(6): 955-965.

664   Hughes M G, Keene J B and Joseph R G. 2000. Hydraulic sorting of heavy-mineral grains by

665   swash on a medium-sand beach. *Journal of Sedimentary Research* **70**(5): 994-1004.

666   Jung S and Hellebrand E. 2006. Trace element fractionation during high-grade metamorphism

667   and crustal melting - constraints from ion microprobe data of metapelitic, migmatitic

668   and igneous garnets and implications for Sm–Nd garnet chronology. *Lithos* **87**: 193-

669   213.

670   Kamber B S, Greig A and Collerson K D. 2005. A new estimate for the composition of

27

671   weathered young upper continental crust from alluvial sediments, Queensland,

672   Australia. *Geochimica et Cosmochimica Acta* **69**(4): 1041-1058.

673   Kamineni D C, Rao A T and Bonardi M. 1991. The Geochemistry of Monazite Types from the

674   Eastern Ghats Granulite Terrain, India. *Mineralogy and Petrology* **45**: 119-130.

675   Kinny P D and Maas R. 2003. Lu–Hf and Sm–Nd isotope systems in zircon. *Reviews in*

676   *Mineralogy and Geochemistry* **53**(1): 327-341.

677   Klemme S, Günther D, Hametner K, Prowatke S and Zack T. 2006. The partitioning of trace

678   elements between ilmenite, ulvospinel,armalcolite and silicate melts with implications

679   for the early differentiation of the moon. *Chemical Geology* **234**: 251-263.

680   Klemme S, Prowatke S, Hametner K and Günther D. 2005. Partitioning of trace elements

681   between rutile and silicate melts: Implications for subduction zones. *Geochimica et*

682   *Cosmochimica Acta* **69**(9): 2361-2371.

683   Komar P D. 2007. The Entrainment, Transport and Sorting of Heavy Minerals by Waves and

684   Currents. pp 3-48. In *Heavy minerals in use* (eds M. A. Mange and D. T. Wright).

685   Elsevier. Developments in Sedimentology, **58**.

686   Komar P D and Wang C. 1984. Processes of selective grain transport and the formation of

687   placers on beaches. *Journal of Geology* **92**(6): 637-655.

688   Korotev R L. 1996. A self-consistent composition of elemental concentration data for 93

689   geochemical reference samples. *Geostandards Newsletter* **20**(2): 217-245.

690   Levchenko E N. 2006. Specific Features of the Mineral Composition of Titanium–Zirconium

691   Placers in Russia. *Lithology and Mineral Resources* **41**(2): 117-136.

692   Liew T C and Hofmann A W. 1988. Precambrian crustal components, plutonic associations,

693   plate environment of the Hercynian Fold Belt of central Europe: Indications from a Nd

694   and Sr isotopic study. *Contributions to Mineralogy and Petrology* **98**: 129-138.

695   McLennan S M. 2001. Relationships between the trace element composition of sedimentary

696   rocks and upper continental crust. *Geochemistry Geophysics Geosystems* **2**(April 20).

697   Melluso L, Lustrino M, Ruberti E, Brotzu P, Gomes C d B, Morbidelli L, Morra V, Svisera D

698   P and d'Amelio F. 2008. Major and trace-element composition of olivine, perovskite,

699   clinopyroxene, Cr-Fe-Ti oxides, phlogopite and host kamafugites and kimberlites, Alto

700   Paranaiba, Brazil. *The Canadian Mineralogist* **46**: 19-40.

701   Mezeme E B, Cocherie A, Faure M, Legendre O and Rossi P. 2006. Electron microprobe

702   monazite geochronology of magmatic events: Examples from Variscan migmatites and

703   granitoids, Massif Central, France. *Lithos* **87**: 276-288.

704   Millot R, Allègre C-J, Gaillardet J and Roy S. 2004. Lead isotopic systematics of major river

705   sediments: a new estimate of the Pb isotopic composition of the Upper Continental

706   Crust. *Chemical Geology* **203**(1-2): 75-90.

707   Monecke T, Bombach G, Klemm W, Kempe U, Götze J and Wolf D. 2000. Determination of

708   Trace Elements in the Quartz Reference Material UNS-SpS and in Natural Quartz

709   Samples by ICP-MS. *Geostandards Newsletter* **24**(1): 73-81.

710   Muñoz M, Pascarelli S, Aquilanti G, Narygina O, Kurnosov A and Dubrovinsky L. 2008.

711   Hyperspectral micro-XANES mapping in the diamond-anvil cell: Analytical procedure

712   applied to the decomposition of (Mg,Fe)-ringwoodite at the upper/lower mantle

713   boundary. *High Pressure Research* **28**: 665-673.

714   Nagy G, Draganits E, Demeny A, Panto G and Arkai P. 2002. Genesis and transformations of

715   monazite, florencite and rhabdophane during medium grade metamorphism:examples

716   from the Sopron Hills, Eastern Alps. *Chemical Geology* **191**: 25-46.

717   Nair A G, Suresh-Babu D S, Damodaran K T, Shankar R and Prabhu C N. 2009. Weathering

718   of ilmenite from Chavara deposit and its comparison with Manavalakurichi placer

719   ilmenite, southwestern India. *Journal of Asian Earth Sciences* **34**: 115-122.

720   Paine M D, Anand R R, Aspandiar M, Fitzpatrick R R and R.Verrall M. 2005. Quantitative

721   heavy-mineral analysis of a pliocene beach placer deposit in southeastern Australia

722   using the autogeosem. *Journal of Sedimentary Research* **75**: 742-759.

723 Paquette J-L, Chopin C and Peucat J-J. 1989. U-Pb zircon, Rb- Sr and Sm-Nd geochronology

724   of high- to very-high-pressure meta-acidic rocks from the western Alps. *Contributions*

725   *to Mineralogy and Petrology* **101**: 280-289.

726 Patchett P J, White W M, Feldmann H, Kielinczuk S and Hofmann A W. 1984. Hafnium/rare

727   earth element fractionation in the sedimentary system and crustal recycling into the

728   Earth's mantle. *Earth and Planetary Science Letters* **69**: 365-378.

729 Patyk-Kara N G. 2002. Placers in the System of Sedimentogenesis. *Lithology and Mineral*

730   *Resources* **37**(5): 429-441.

731 Patyk-Kara N G. 2008. Sedimentogenesis and Placer Formation. *Lithology and Mineral*

732   *Resources* **43**(4): 318-325.

733 Patyk-Kara N G and Shevelev A G. 2000. Inhomogeneity of the Mineral Field of Complex

734   Polymineral Placers. *Lithology and Mineral Resources* **35**(2): 109-120.

735 Peucat J J, Jegouzo P, vidal P and Bernard-Griffiths J. 1988. Continental crust formation seen

736   through the Sr and Nd isotope systematics of S-type granites in the Hercynian belt of

737   western France. *Earth and Planetary Science Letters* **88**: 60-68.

738 Pin C and Duthou J-L. 1990. Sources of Hercynian granitoids from the French Massif Central:

739   Inferences from Nd Isotopes and consequences for crustal evolution. *Chemical Geology*

740   **83**(3/4): 281-296.

741 Preston J, Hartley A, Mange-Rajetzky M, Hole M, May G, Buck S and Vaughan L. 2002. The

742   provenance of triassic continental sandstones frome the Beryl field, northern north sea:

743   Mineralogical, geochemical and sedimentological constraints. *Journal of Sedimentary*

744   *Research* **72**(1): 18-29.

745 Radulescu I G, Rubatto D, Gregory C and Compagnoni R. 2009. The age of HP metamorphism

746   in the Gran Paradiso Massif, Western Alps: A petrological and geochronological study

747   of "silvery micaschists". *Lithos* **110**(95-108).

748   Rao B N. 1994. Significance of heavy mineral ratios in some beach placers of Andhra Pradesh,

749   East Coast of India. *Current Science* **67**(7): 535-537.

750   Rossi P, Cocherie A, Fanning C M and Deloule E. 2006. Variscan to eo-Alpine events recorded

751   in European lower-crust zircons sampled from the French Massif Central and Corsica,

752   France. *Lithos* **87**: 235-260.

753   Roy P S. 1999. Heavy Mineral Beach Placer in Southeastern Australia: Their Nature and

754   Genesis. *Economic Geology* **94**: 567-588.

755   Rudnick R L and Gao S. 2003. Composition of the Continental Crust. pp 1-64. In *The Crust*

756   (ed. R.L. Rudnick) *Vol. 3, Treatise on Geochemistry* (eds. H.D. Holland and K.K.

757   Turekian), Elsevier-Pergamon, Oxford.

758   Sabatier F, Maillet G, Provansal M, Fleury T-J, Suanez S and Vella C. 2006. Sediment budget

759   of the Rhône delta shoreface since the middle of the 19th century. *Marine Geology* **234**:

760   143-157.

761   Sergeev S A, Meier M and Steiger R H. 1995. Improving the resolution of single-grain U/Pb

762   dating by use of zircon extracted from feldspar: Application to the Variscan magmatic

763   cycle in the central Alps. *Earth and Planetary Science Letters* **134**: 37-51.

764   Steinmann M and Stille P. 2008. Controls on transport and fractionation of the rare earth

765   elements in stream water of a mixed basaltic–granitic catchment basin (Massif Central,

766   France). *Chemical Geology* **254**: 1-18.

767   Strnad L, Ettler V, Mihaljevic M, Hladil J and Chrastny V. 2009. Determination of Trace

768   Elements in Calcite Using Solution and Laser Ablasion ICP-MS: Calibration to NIST

769   SRM Glass and USGS MACS Carbonate, and Application to Real Landfill Calcite.

770   *Geostandards Newsletter* **33**(3): 347-355.

771   Suresh-Babu D S, Thomas K A, Mohan-Das P N and Damodaran A D. 1994. Alteration of

772   ilmenite in the Manavalakurichi deposit, India. *Clays and Clay Minerals* **42**(5): 567-

773   571.

774   Taylor S R and McLennan S M. 1995. The Geochemical evolution of the continental crust.

775   *Reviews of Geophysics* **33**(2): 241-265.

776   Thomassin A, Blanchardon E, Bottolier-Depois J-F, Bouisset P, Cagnat X, Chazel V, Clairand

777   I, Frelon S, Gurriaran R, Huet C, Paquet F, Pourcelot L and Tourlonias E. 2007.

778   Evaluations dosimétriques de l'exposition potentielle liée à l'accumulation naturelle

779   d'uranium et de thorium dans les sables de certaines plages du littoral de Camargue.

780   *Rapport IRSN n°2007/01*.

781   Thöni M, Miller C, Zanetti A, Habler G and Goessler W. 2008. Sm–Nd isotope systematics of

782   high-REE accessory minerals and major phases: ID-TIMS, LA-ICP-MS and EPMA

783   data constrain multiple Permian–Triassic pegmatite emplacement in the Koralpe,

784   Eastern Alps. *Chemical Geology* **254**: 216-237.

785   Tilton G R, Schreyer W and Schertl H-P. 1991. Pb-Sr-Nd isotopic behavior of deeply subducted

786   crustal rocks from the Dora Maira Massif, Western Alps, Italy-II: What is the age of the

787   ultrahigh-pressure metamorphism? *Contributions to Mineralogy and Petrology* **108**: 22-

788   33.

789   Totten M W and Hanan M A. 2007. Heavy Minerals in Shales. pp. 323-343. In *Heavy mineral*

790   *in use (eds* M. A. Mange and D. T. Wright). Elsevier. Developments in Sedimentology,

791   **58**.

792   Vassas C, Pourcelot L, Vella C, Carpéna J, Pupin J P, Bouisset P and Guillot L. 2006.

793   Mechanisms of enrichment of natural radioactivity along the beaches of the Camargue,

794   France. *Journal of Environmental Radioactivity* **91**: 146-159.

795   Vella C, Fleury T-J, Raccasi G, Provansal M, Sabatier F and Bourcier M. 2005. Evolution of

796   the Rhône delta plain in the Holocene. *Marine Geology* **222–223**: 235-265.

797   Vervoort J D and Blichert-Toft J. 1999. Evolution of the depleted mantle: Hf isotope evidence

798   from juvenile rocks through time. *Geochimica et Cosmochimica Acta* **63**(3/4): 533-556.

799   Vervoort J D and Jonathan Patchett P. 1996. Behavior of hafnium and neodymium isotopes in

800   the crust: Constraints from Precambrian crustally derived granites. *Geochimica et*

801   *Cosmochimica Acta* **60**(19): 3717-3733.

802   Vervoort J D, Patchett P J, Albarède F, Blichert-Toft J, Rudnick R and Downes H. 2000. Hf-

803   Nd isotopic evolution of the lower crust. *Earth and Planetary Science Letters* **181**(1-2):

804   115-129.

805   Vervoort J D, Patchett P J, Blichert-Toft J and Albarède F. 1999. Relationships between Lu–

806   Hf and Sm–Nd isotopic systems in the global sedimentary system. *Earth and Planetary*

807   *Science Letters* **168**: 79–99.

808   Vervoort J D, Patchett P J, Gehrels G E, and Nutman A P. 1996. Constraints on early Earth

809   differentiation from hafnium and neodymium isotopes. *Nature* **379:** 624–627.

810   Zhu X K and O'Nions R K. 1999. Monazite chemical composition: some implications for

811   monazite geochronology. *Contributions to Mineralogy and Petrology* **137**: 351-363.

812

813

814

816   *Figure 1*: **Location map of the studied area in France.** The massifs drained by the

817   Rhone river and its tributaries are indicated in map (a). The sampling site of the Camargue

818   placer and the sediment transport direction alongside the coast are shown in the inset (b).

819   Figure 1

820
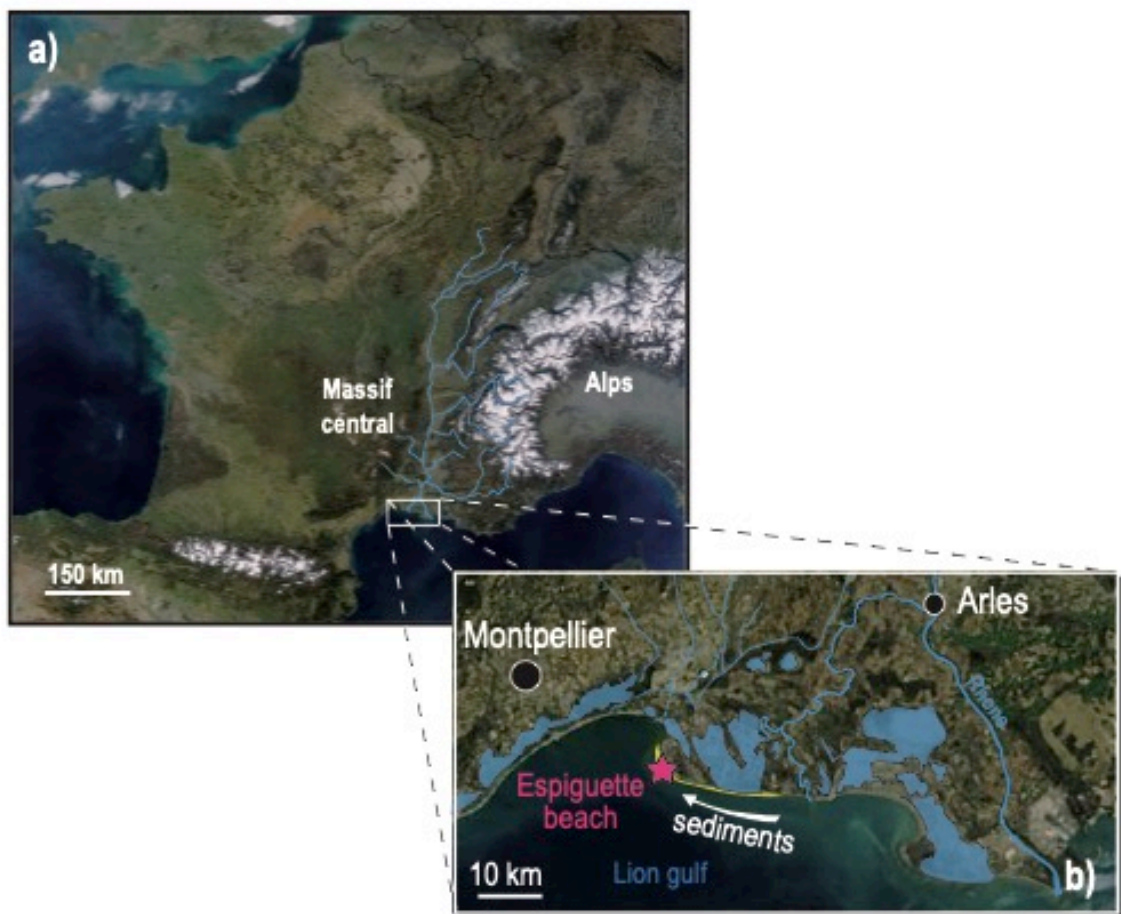
821   *Figure 2*: **Mineral abundances in the heavy fraction (d>2.9).** A picture of the heavy

822   fraction and the mineral proportions estimated as a percentage of the total grains counted under

823   the binocular microscope are reported in the bottom left corner. The μ-XRF mapping showing

824   the mineral species of the analysed grains on the adhesive surface and the mineral abundances

825   calculated using this method as a percentage of the counted grains are presented in the top right

826   corner. The heavy mineral abundances determined by combining the results from both methods

827   are shown in the grey-coloured inset as a percentage of the total counted grains and as a mass

828   percentage. For mass percentage calculations, we used the characteristic mineral densities given

829   by Deer et al. (1992) and we estimated, based on binocular microscope observations, that all

830   the grains had roughly the same volume except for the epidote and titanite for which the radius

831   were considered to be 1.5 times larger than that of the other grains. Taking into account all

832   sources of errors, the uncertainties on the mass percentages are estimated at about 3%.

833   **Figure 2**

834
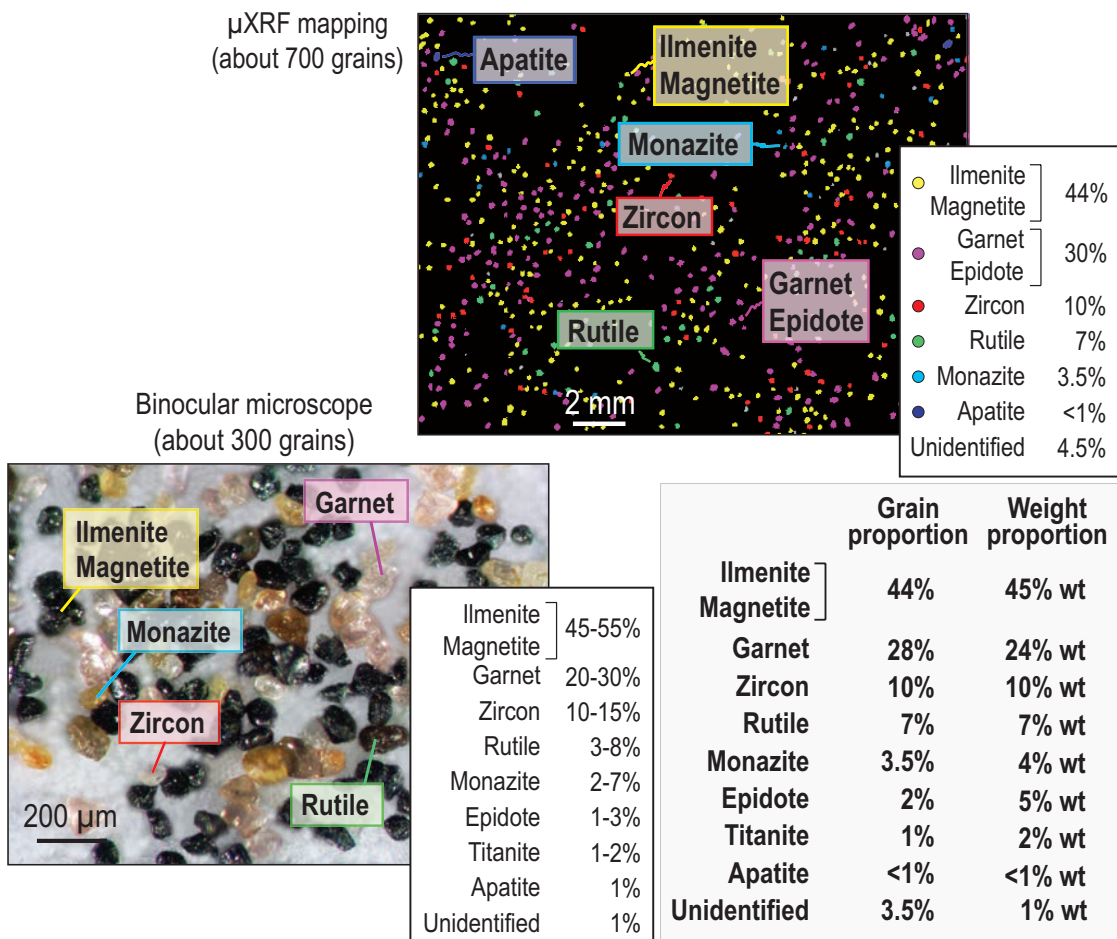
Figure 3: **REE and trace elements in the mineral fractions isolated from the**

Camargue placer. (a) REE patterns normalized to the average composition of chondrites as

given by Evensen et al. (1978). (b) Trace element patterns normalized to the average

composition of the upper continental crust given by McLennan (2001).
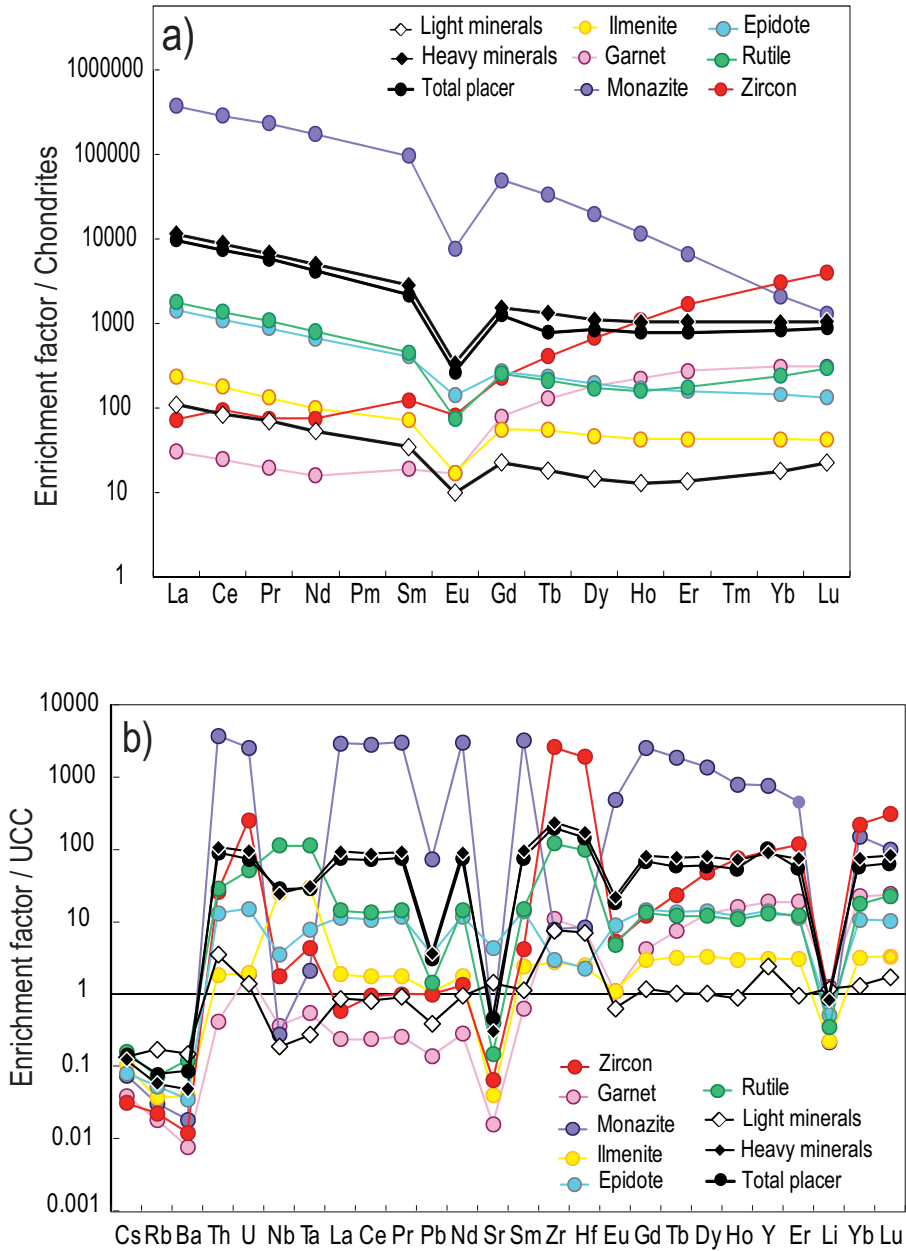
Figure 3

841   *Figure 4:* **Nd and Hf isotopes in the mineral fractions isolated from the Camargue**

842   **placer.** The mantle array is that defined by Chauvel et al. (2008) associated with the CHUR

843   composition given by Bouvier et al. (2008). The proportions of monazite (f_{Mnz}) in the binary

844   mixing between zircon and monazite are shown by ticks on the mixing hyperbola connecting

845   the two endmembers. The proportions of monazite in the point of maximum curvature of the

846   mixing hyperbola are shown in more detail in the inset. Continental crust rock data are from

847   Bennett et al. (1993), Vervoort et al. (1996), Vervoort and Patchett (1996), Vervoort and

848   Blichert-Toft (1999) and Vervoort et al. (2000) and plot along an array of $\varepsilon_{Hf} = 1.50 \times \varepsilon_{Nd} - 0.60$.

849   Note that this Nd-Hf relation has the same slope as the mantle array of Chauvel et al. (2008)

850   but passes below the BSE value defined by Bouvier et al. (2008). Analytical errors are smaller

851   than the symbol size.

852   Figure 4

853
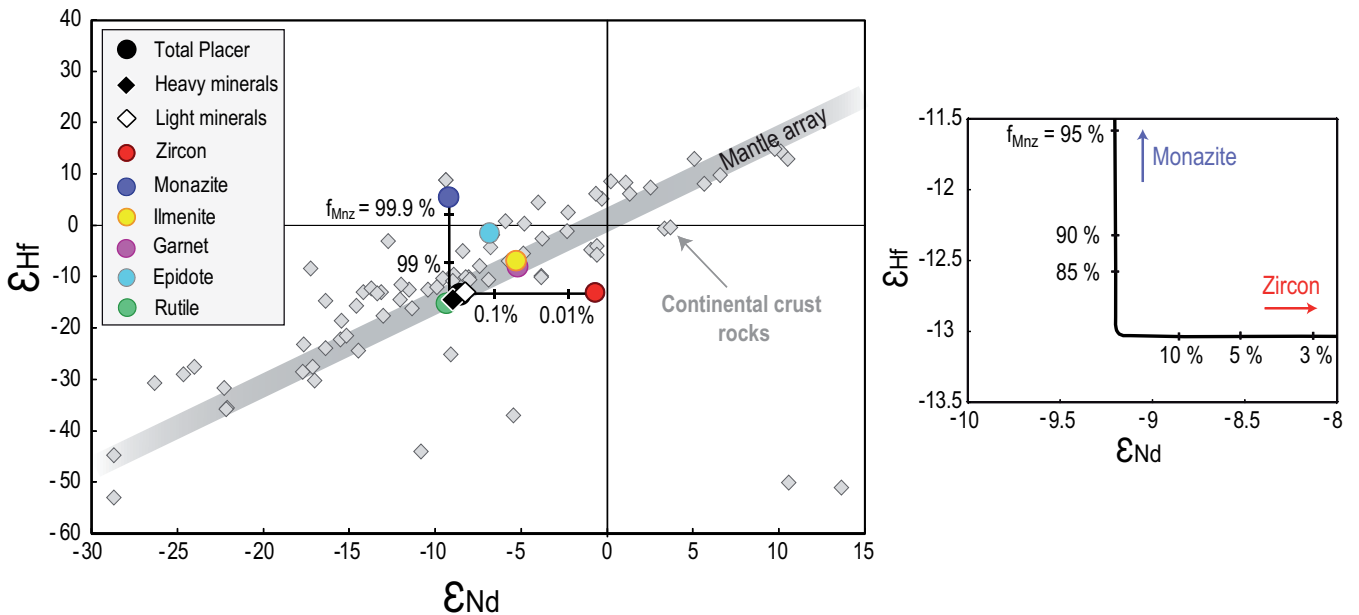
854   *Figure 5:* **Trace-element patterns of the mineral fractions normalised to the**

855   **composition of the Camargue placer.**

856   Figure 5

857
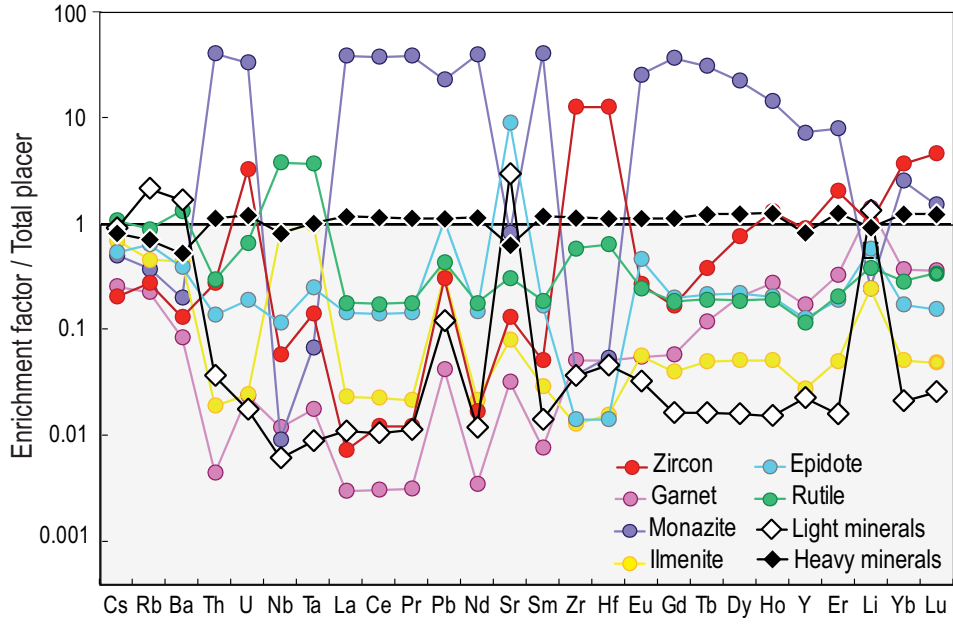
858   *Figure 6:* **Modelling of the heavy-mineral trace-element pattern.** The concentrations

859   in the heavy mineral fraction were modelled by summing the concentrations of the pure mineral

860   separates multiplied by their mass proportions (estimates done under the binocular microscope

861   and using the μ-XRF method for each mineral - see Figure 2). To take into account the

862   uncertainties on mineral percentages, the proportion of the different phases was taken as

863   variable within 2 limits: ilmenite + magnetite: 42 - 48 wt%, garnet: 21 - 27 wt%, zircon: 8 – 12

864   wt%, rutile: 5 - 9 wt%, epidote: 3 - 7 wt% and monazite: 2 - 6 wt%. The blue field represents

865   the entire range of modelled patterns obtained by sampling different mineral proportions within

866   the ranges of values given above.

867

868
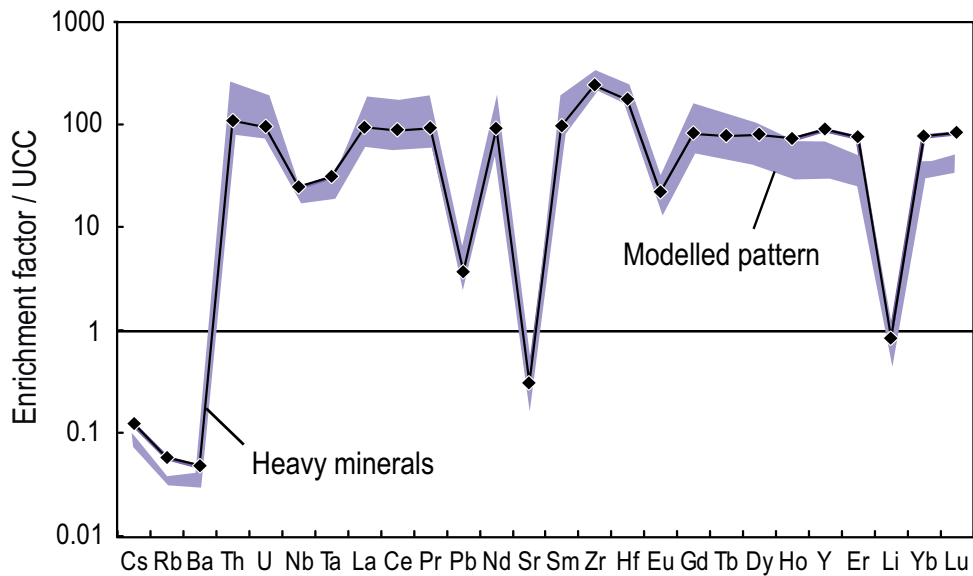
Figure 6

869   *Figure 7*: **Histogram of ε_{Nd} values for crustal rocks from the Massif Central and the**

870   **Alps**. Whole-rock Nd isotope data are from Downes (1984), Bossard et al. (1986), Downes and

871   Duthou (1988), Paquette et al. (1989), Pin and Duthou (1990), Tilton et al. (1991), Downes et

872   al. (1997), Duchene et al. (1997), Henry et al. (1997) and Steinmann and Stille (2008). ε_{Nd} values

873   are calculated using the CHUR composition of Bouvier et al. (2008).

874   Figure 7

875
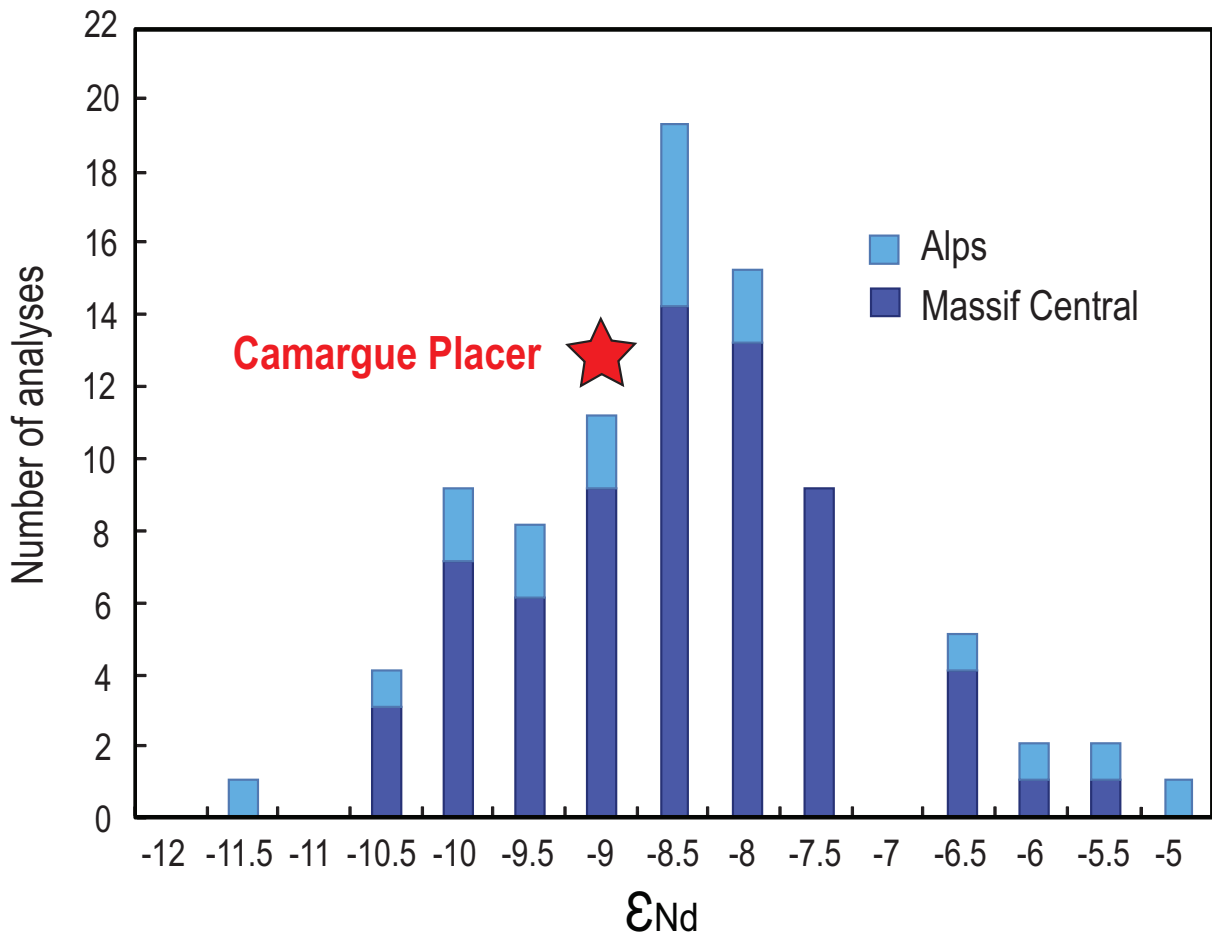
876   *Figure 8:* **Sketch of Hf two stage model age calculations.** CC: Continental crust. mx:

877   mineral. T_{DM}: Hf two stage model age (extraction time from the depleted mantle). t_c:

878   crystallisation age of the mineral.

879   # Figure 8

880
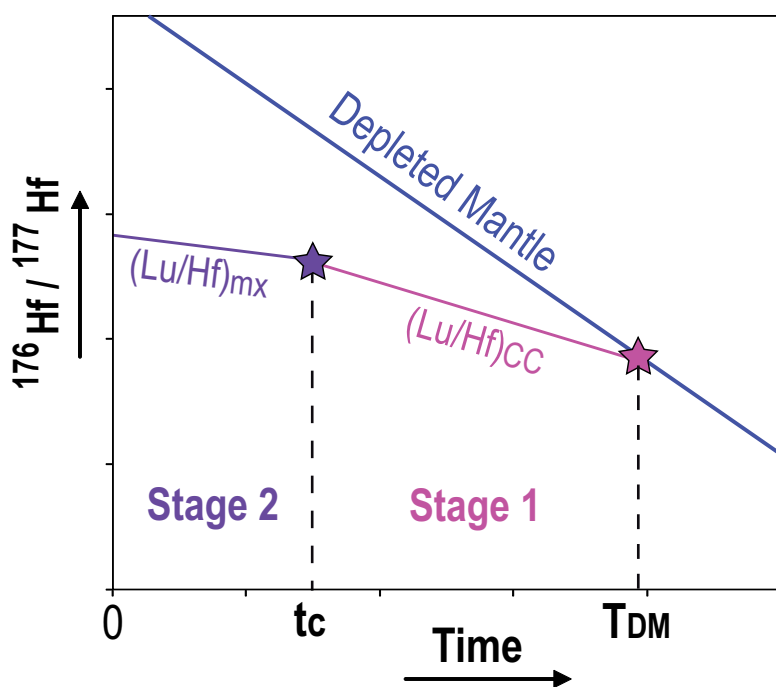
Figure 9: **Hf model ages versus Nd model ages obtained from 10 000 Monte Carlo**

882 **simulations.** As illustrated in Figure 8, model ages were calculated using two stages and the

883 following equation (here for Hf):

884
$$T_{DM}=t_c+\frac{1}{\lambda_{Hf}}\ln\left[\frac{\left(^{176}Hf/_{177}Hf\right)_{mx}^{t_c}-\left(^{176}Hf/_{177}Hf\right)_{DM}^{t_c}}{\left(^{176}Lu/_{177}Hf\right)_{CC}^{t_c}-\left(^{176}Lu/_{177}Hf\right)_{DM}^{t_c}}+1\right]$$

885 The acronyms used in this equation are similar to those of Figure 8. All the model ages

886 were calculated using a Monte-Carlo procedure (n=10 000 for each mineral fraction and for the

887 placer) to propagate the input parameter uncertainties. The distribution of crystallisation ages

888 (t_c) follows a Gaussian law with a mean value of 300 Ma and a standard deviation (2σ) of 50

889 Ma. After having randomly sampled a crystallisation age in the latter distribution,

890 $\left(^{143}Nd/_{144}Nd\right)_{DM}^{t_c}$, $\left(^{147}Sm/_{144}Nd\right)_{DM}^{t_c}$, $\left(^{176}Hf/_{177}Hf\right)_{DM}^{t_c}$ and $\left(^{176}Lu/_{177}Hf\right)_{DM}^{t_c}$ were calculated using the

891 following parameters: (a) we assume that the depleted mantle has linearly evolved from a bulk

892 Earth value at Earth formation, (b) we use the CHUR values published by Bouvier et al. (2008)

893 and (c) we sample randomly the $\left(^{143}Nd/_{144}Nd\right)_{DM}^{0}$ and $\left(^{176}Hf/_{177}Hf\right)_{DM}^{0}$ isotopic ratios in Gaussian

894 distributions centered at the mean-MORB pole of Chauvel et al. (2008) with a standard

895 deviation (2σ) of 2ε units. $\left(^{143}Nd/_{144}Nd\right)_{mx}^{t_c}$ and $\left(^{176}Hf/_{177}Hf\right)_{mx}^{t_c}$ were calculated back in time

896 using the Nd and Hf isotopic ratios and the Lu, Hf, Sm and Nd concentrations measured in this

897 study. Finally, $\left(^{147}Sm/_{144}Nd\right)_{CC}^{t_c}$ and $\left(^{176}Lu/_{177}Hf\right)_{CC}^{t_c}$ were calculated using $\left(^{147}Sm/_{144}Nd\right)_{CC}^{0}$ and

898 $\left(^{176}Lu/_{177}Hf\right)_{CC}^{0}$ ratios randomly sampled in Gaussian distributions centered at 0.115 ± 0.005 (2σ)

899 and 0.013 ± 0.004 (2σ), respectively (values from McLennan, 2001 and Rudnick and Gao,

900 2003). $\lambda_{Nd} = 6.54*10^{-12}$ yr^{-1} and $\lambda_{Hf} = 1.87*10^{-11}$ yr^{-1}. For each mineral fraction and for the placer,

901 colour dots show the location of model ages as calculated using the Monte Carlo simulation.

902 The distribution of Nd and Hf model ages for all fractions together, are shown as histograms

903 along the x and y axes.
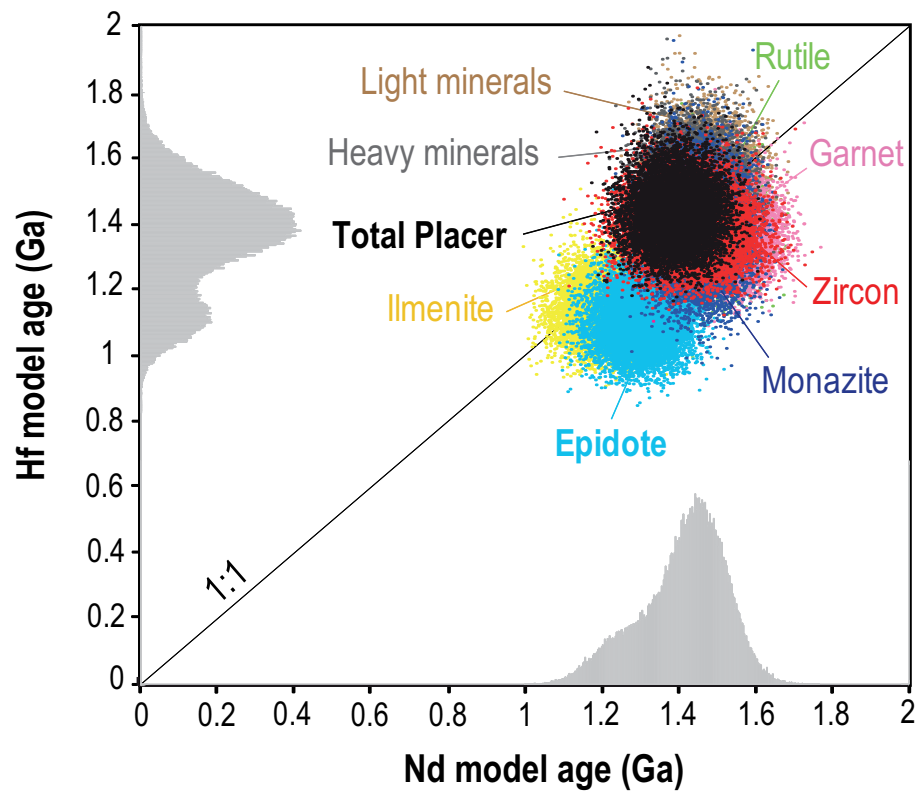
905   **Tables**

906   *Table 1:* **Trace-element concentrations measured in the various fractions (ppm).**

907   Concentrations were calibrated to the BR standard composition using the reference values

908   recommended by Eggins et al. (1997). Precision on the measured concentrations of most

909   elements is usually better than 5% as described in details by Chauvel et al. (2011) and values

910   obtained for the rock standards analysed as unknown samples are similar to published values

911   within 3% (see Supplementary Table 2).

912

913

Table 1: Trace-element concentrations measured in the various fractions (ppm)

Sample	CAM Mnz	CAM Grt	CAM Il	CAM Zr	CAM Ru	CAM Ep	CAM HMC	CAM fd NT	Plac7
Description	Monazite	Garnet	Ilménite	Zircon	Rutile	Epidote	Heavy minerals d > 2.9	Light minerals d < 2.9	Total placer
Li	4.49	25.6	4.45	18.4	7.04	10.5	16.7	24.2	17.9
Rb	3.48	2.09	4.22	2.53	8.23	5.95	6.53	19.9	9.09
Sr	143	5.6	14.1	23	53.5	1525	108	509	170
Y	17419	414	68.1	2137	285	313	1969	55.5	2363
Zr	1509	2090	528	501294	23353	581	45508	1494	39432
Nb	3.44	4.44	303	21.5	1366	42.7	295	2.29	360
Cs	0.356	0.181	0.489	0.145	0.749	0.379	0.572	0.643	0.694
Ba	10.3	4.32	22.5	6.7	67.2	19.7	26.7	85	50
La	90255	7.28	56.7	17.7	433	350	2788	26.7	2345
Ce	182339	15.4	113	60.6	866	699	5635	53	4833
Pr	22283	1.87	12.8	7.19	104	84.6	652	6.69	569
Nd	80352	7.42	46.2	35.2	374	312	2363	25.2	2039
Sm	14649	2.85	11	18.9	68.7	62.6	432	5.27	360
Eu	439	0.96	0.987	4.69	4.3	8.09	19.4	0.571	17
Gd	9927	16	11.3	59.9	52.9	55	324	4.66	271
Tb	1227	4.79	2.05	15.3	7.87	8.66	49.5	0.673	39.7
Dy	4968	46.1	11.7	171	42.8	49.4	279	3.66	221
Ho	656	12.7	2.4	60.1	8.9	9.6	58	0.725	45.5
Er	1081	44.6	7.09	276	28.6	26.5	173	2.23	135
Yb	344	50.6	7.05	495	39.1	23.6	168	2.94	134
Lu	33	7.78	1.07	99.5	7.38	3.37	26.6	0.569	21.3
Hf	50	47	14.6	11230	579	13.1	1012	42.2	889
Ta	2.14	0.549	30.2	4.4	113	7.8	31	0.28	30.3
Pb	1268	2.38	18.4	17.2	24.5	60.5	62.7	6.87	55.3
Th	40663	4.58	20.1	284	306	142	1154	38.2	1006
U	7233	5.33	5.54	720	146	42.4	265	3.96	217

914   ***Table 2:* Nd and Hf isotopic compositions of various fractions.** *Re-run* stands for run

915   duplicates. Uncertainties (± 2σ) reported in the Table correspond to in-run errors. Nd and Hf

916   isotopes were calculated relative to the Ames-Rennes Nd and Ames-Grenoble Hf standard

917   values given by Chauvel and Blichert-toft (2001) and Chauvel et al. (2011) (^{143}Nd/^{144}Nd =

918   0.511961 ± 13 (2σ) and ^{176}Hf/^{177}Hf = 0.282160 ± 12 (2σ)). The reproducibility calculated using

919   re-run analyses and duplicates (see Supplementary Table 3) is 0.000013 (2σ, n=7) for the

920   ^{176}Hf/^{177}Hf ratios and 0.000037 (2σ, n=7) for the ^{143}Nd/^{144}Nd ratios. ε_{Nd} and ε_{Hf} are calculated using

921   the CHUR composition given by Bouvier et al. (2008). Considering the reproducibility of the

922   entire analytical procedure, uncertainties are estimated at ± 0.7 ε units for ε_{Nd} and ε_{Hf} values.

Table 2: Nd and Hf isotopic compositions of various fractions

Sample	Description	$^{143}Nd/^{144}Nd$	± 2σ	ε$_{Nd}$	$^{176}Hf/^{177}Hf$	± 2σ	ε$_{Hf}$
CAM Mnz	*Monazite*	0.512158	± 9	-9.2	0.282942	± 9	+5.6
CAM Mnz Re-run		0.512166	± 7	-9.0			
CAM Grt	*Garnet*	0.512363	± 9	-5.2	0.282559	± 6	-8.0
CAM Il	*Ilmenite*	0.512359	± 8	-5.3	0.282593	± 7	-6.8
CAM Il Re-run		0.512390	± 7	-4,7			
CAM Zr	*Zircon*	0.512594	± 5	-0.7	0.282417	± 5	-13.0
CAM Zr Re-run					0.282409	± 6	-13.3
CAM Ru	*Rutile*	0.512150	± 13	-9.4	0.282358	± 5	-15.1
CAM Ep	*Epidote*	0.512279	± 5	-6.9	0.282743	± 19	-1.5
CAM HMC	*Heavy minerals d>2,9*	0.512169	± 5	-9.0	0.282374	± 5	-14.5
CAM HMC Re-run		0.512183	± 9	-8,7	0.282378	± 6	-14.4
CAM fd NT	*Light minerals d<2,9*	0.512181	± 8	-8.8	0.282440	± 5	-12.2
CAM fd NT Re-run					0.282441	± 7	-12.2
Plac7	*Total placer*	0.512190	± 10	-8.6	0.282406	± 11	-13.4

		$^{143}Nd/^{144}Nd$	± 2σ	ε$_{Nd}$	$^{176}Hf/^{177}Hf$	± 2σ	ε$_{Hf}$

Supplementary File A

Determination of heavy mineral abundances by micro X-ray fluorescence

Several hundred grains were laid down on an adhesive surface and mapped by micro X-ray fluorescence (μXRF EDAX Eagle III) to identify spectral signatures that are characteristic for each mineralogical phase. The analyses were performed under primary vacuum with a 50μm X-ray spot size on a 512x400 pixel grid. Spectra were acquired on each pixel with a dwell time of 400 ms and a sampling step of 50 μm in x and y. On the adhesive surface, the grains were previously spaced at distances of at least 50μm from each other to insure better recognition of the spectral signature of each grain. X-ray tube operating conditions were maintained at 20 kV and 200 μA during all analyses. In the heavy mineral fraction (d > 2.9), the mineral species were discriminated using the X-ray fluorescence energies (K_α, K_β, L_α or L_β) of ten chemical elements (Si, Al, Ca, P, Zr, Ti, Fe, Mn, Nd and Ce) on a 0-20 KeV energy range. Among all spectra, we selected some representative reference spectra for the background noise and for each mineral of interest (ilmenite, magnetite, zircon, garnet, monazite and rutile). As used by Muñoz et al. (2008) for micro-XANES mapping, our computer code then determines the best linear combination of reference spectra that reproduces the intensities measured by μXRF for the chosen chemical elements and for each pixel. If one of the linear coefficients is close to 1, the computer code associates the pixel with the corresponding mineral species (or the background); if not, the pixel is considered to be unidentified. Then, using this information and standard image processes, we created a map showing the nature of almost all the grains analysed by μXRF and we calculate the relative abundance of each referenced mineral species as a percentage of the total grains analysed on the adhesive surface.

Supplementary File B

Sample dissolution

Because placer minerals are quite difficult to dissolve at 150°C in bombs, only few mg of each mineral fraction were dissolved in acid mixtures combining pure concentrated HF, HCl, $HClO_4$ and HNO_3 (see Table B.1). For the six pure and homogeneous mineral fractions, we dissolved the quantity required to measure both trace element concentrations and Nd-Hf isotopic ratios. In contrast, for the total placer and the two fractions of light and heavy minerals, we dissolved about 30 to 50 mg of powders to minimize heterogeneities and obtain representative analyses.

Trace element concentrations

To measure trace element concentrations similar to those of the BR rock standard (external calibration), samples were diluted about 5000 times before being analysed on the ICP-MS. In contrast, when trace element concentrations were unusually high compared to the BR rock standard (Hf in zircons, REE in monazites, etc...), high dilution factors were preferentially used to calculate precise concentrations (see Table B.1). In that case, the dilution procedure was performed in several steps by carefully weighing the mass of each aliquot taken from the "mother" solution. Several procedural duplicates were then analysed to evaluate the reproducibility of the entire dilution procedure.

Chemical separation of Hf in the pure mineral fractions

Even if the dissolved quantity of sample powder was initially low (few mg), our calculations show that the resin used for the second Hf column would be saturated if we loaded some of the pure mineral separates on a column filled with 2 mL of anionic resin. To avoid resin-saturation problems that may cause loss of Hf, the standard Hf isolation procedure

described by Blichert-toft et al. (1997) and modified by Chauvel et al. (2011) was adapted to each of the mineral fractions. For the rutile, monazite and zircon separates, the second Hf step that separates Hf from some major elements was removed because (1) these minerals do not contain high amount of these major elements and (2) there is a high risk to loose Hf during this step. For the epidote, garnet and ilmenite fractions, we kept the second Hf column because these minerals may contain significant amount of Fe, Ca or Al that need to be isolated from Hf to insure high precision on the Hf-isotope measurements (see Table B.1). However, to perform this step without saturating the resin, the ilmenite fraction was divided in two fractions loaded on two different columns that were subsequently merged to finish the chemical separation.

Table B.1 : **Sample-specific analytical procedures**

Sample	Description	Sample Dissolution			Trace element analyses	Hf isolation
		Dissolved Quantity	Acid mixtures	Time in bombs	Dilution factor	Second Hf column
Plac7	Total placer	≈ 50 mg	HF-HClO$_4$-HNO$_3$	2 months	10000	x
CAM HMC	Heavy minerals	≈ 35 mg	HF-HClO$_4$-HCl-HNO$_3$	2 months	500 000 for REE, U, Th, Y, Hf, Zr 5000 for the other elements	x
CAM fd NT	Light minerals	≈ 35 mg	HF-HClO$_4$-HNO$_3$	1 month	5000	x
CAM Mnz	Monazite	≈ 35 mg	HF-HCl-HNO$_3$	3 weeks	1 000 000 for REE, U, Th, Y 5000 for the other elements	
CAM Zr	Zircon	≈ 10 mg	HF-HClO$_4$-HCl-HNO$_3$	2 months	5 000 000 for Hf and Zr 5000 for the other elements	
CAM Ru	Rutile	≈ 5 mg	HF-HClO$_4$-HNO$_3$	3 weeks	5000	
CAM Il	Ilmenite	≈ 30 mg	HF-HClO$_4$-HCl-HNO$_3$	3 weeks	5000	x
CAM Grt	Garnet	≈ 10 mg	HF-HClO$_4$-HCl	2 weeks	40 000 for REE 5000 for the other elements	x
CAM Ep	Epidote	≈ 5 mg	HF-HClO$_4$-HCl	2 weeks	5000	x

Supplementary Table 1: Heavy minerals identified in Espiguette black-sands (modified after BRGM, 2000)

Heavy minerals	Abundance
Amphibole	L
Apatite	R
Biotite	R
Carbonates	L
Chlorite	R
Disthene	R
Epidote	A
Garnet	A
Ilmenite	L
Iron hydroxides	L
Leucoxene	R
Magnetite	L
Monazite	R
Pyroxene	L
Rutile	R
Sillimanite	R
Spinel	R
Staurotide	R
Titanite	R
Tourmaline	R
Zircon	R

R: Rare
L: Low content
A: Abundant

Supplementary Table 2: Trace-element concentrations in rock standards

	BR ref *Eggins et al. (1997)*	AGV-1 n=4	2σ (%)	AGV-1 *Eggins et al. (1997)*	Diff (%)	BR 24 n=4	2σ (%)	BR 24 *LGCA values*	Diff (%)
Li	14.9	11.0	0.8	11.2	2.0	7.17	1.6	7.06	-1.6
Rb	48.7	69.9	0.4	68.3	-2.4	84.6	1.2	83.67	-1.1
Sr	1364	674	1.2	655	-2.9	619	1.8	618.71	-0.1
Y	31.5	21.1	0.8	21	-0.5	30.9	0.6	30.96	0.2
Zr	283	244	1.3	240	-1.8	302	2.0	303.5	0.6
Nb	119	14.8	4.4	14.9	0.7	40.2	3.4	39.6	-1.5
Cs	0.823	1.31	2.2	1.31	-0.1	0.662	3.4	0.65	-1.9
Ba	1082	1220	3.4	1223	0.1	394	2.0	387.29	-1.7
La	82.1	38.4	0.8	38.5	0.2	34.0	0.8	33.43	-1.6
Ce	152	69.0	0.2	68.5	-0.7	73.3	1.6	72.66	-0.9
Pr	17.4	8.53	0.4	8.45	-0.9	9.63	1.4	9.59	-0.5
Nd	66.1	31.9	0.9	31.6	-1.1	39.8	1.4	39.67	-0.3
Sm	12.1	5.86	0.9	5.82	-0.6	8.33	2.2	8.33	0.0
Eu	3.58	1.59	3.0	1.57	-1.3	2.5	1.2	2.48	-0.7
Gd	9.57	4.62	1.8	4.73	2.3	7.41	1	7.32	-1.2
Tb	1.29	0.65	2.3	0.664	2.1	1.08	2.8	1.06	-1.5
Dy	6.3	3.53	2.9	3.54	0.2	5.68	1.8	5.67	-0.2
Ho	1.09	0.678	1.7	0.69	1.7	1.05	2.2	1.06	0.6
Er	2.59	1.84	3.1	1.86	0.8	2.72	1.2	2.71	-0.5
Tm									
Yb	1.81	1.63	1.3	1.64	0.8	2.09	0.4	2.09	-0.2
Lu	0.251	0.249	3.1	0.248	-0.3	0.303	3.4	0.3	-1.0
Hf	5.62	5.00	1.3	5	0.1	6.62	1.2	6.69	1.0
Ta	5.79	0.865	1.5	0.882	1.9	2.46	1	2.44	-0.9
Pb	4.77	37.5	1.1	37.3	-0.7	3.75	0.8	3.69	-1.7
Th	10.9	6.47	0.9	6.53	0.9	4.84	1.6	4.83	-0.1
U	2.46	1.9	1.7	1.89	-0.8	1.22	1.6	1.23	1.0

Standard deviations (2σ) were calculated between the n measurement compositions of the two rock standards analysed as unknown samples and calibrated to the BR standard using the reference values given in the first column of this Table. Differences between the published values and our measurement compositions (Diff) are also reported.

Supplementary Table 3: Trace-element concentrations and Nd-Hf isotopic compositions of the impure fractions

Sample	CAM Mnz NT	CAM Mnz NT Re-run	CAM Grt NT	CAM Grt NT Dup	CAM Il NT	CAM Il NT Dup	CAM Zr NT	CAM Zr NT Re-run	CAM Zr NT Proc Dup
Description	Impure Monazites	Impure Monazites	Impure Garnets	Impure Garnets	Impure Ilmenites	Impure Ilmenites	Impure Zircons	Impure Zircons	Impure Zircons
Li	35.9		20.9	21.4	5.06		16.8		
Rb	10.3		3.47	3.3	4.16		2.97		
Sr	631		12.3	11.4	12.8		24.3		
Y	7038		359	359	33.9		1443		
Zr	1066		190	176	332		388303		
Nb	492		66.4	58.1	265		252		
Cs	1.62		0.369	0.382	0.474		0.188		
Ba	37.5		14.1	12.3	21.8		148		
La	33617		54.5	38.1	45		16.6		
Ce	69266		105	75.6	92.7		47.4		
Pr	8223		11.7	8.49	10.1		5.64		
Nd	29906		39.7	29.3	35.6		25.2		
Sm	5397		8.3	7.13	6.61		13		
Eu	201		1.19	1.16	0.592		3.47		
Gd	3513		17.8	18	5.62		34		
Tb	432		4.54	4.69	0.943		8.62		
Dy	1765		41.9	42.1	5.65		86.4		
Ho	232		11	11.1	1.18		46.2		
Er	421		38.5	38.6	3.68		207		
Yb	173		44.1	44.1	3.89		364		
Lu	19		6.79	6.76	0.613		73.5		
Hf	31.1		4.69	4.52	8.66		8818		
Ta	114		8.79	5.93	25.9		16.7		
Pb	422		16.7	14.6	18.5		15.4		
Th	34991		19	14.7	17.7		194		
U	2213		3.75	4.77	4.63		635		
143Nd/144Nd	0.512146	0.512158	0.512294	0.512350	0.512264	0.512274	0.512509		0.512505
± 2σ	± 6	± 6	± 7	± 8	± 8	± 6	± 5		± 6
εNd	-9.4	-9.2	-6.6	-5.5	-7.1	-6.9	-2.4		-2.4
176Hf/177Hf	0.282984		0.283656	0.283670	0.282582	0.282603	0.282375	0.282384	0.282382
± 2σ	± 22		± 15	± 8	± 7	± 12	± 7	± 6	± 7
εHf	7.0		30.8	31.3	-7.2	-6.4	-14.5	-14.2	-14.3

Trace-element concentrations (ppm) and Hf-Nd isotopic compositions measured in monazite, garnet, ilmenite and zircon fractions before their purification by handpicking under a binocular microscope. Concentrations were obtained in the same way as for their respective pure mineral separates. The two dissolutions of the impure garnet fraction are not very reproducible most probably because of sample heterogeneity (unpurified fraction with a complex mineral assemblage). **Dup:** dissolution duplicate. **Proc Dup:** analytical procedure duplicate. **Re-run:** run duplicate